AD-A078 547 OPERATION TUMBLER NEVADA PROVING GROUNDS APRIL-JUNE 1952 PROJECT 14 AIR BLAST MEASUREMENTS(U) ARMY BALLISTIC RESEARCH LAB ABERDEEN PROVING GROUND MD

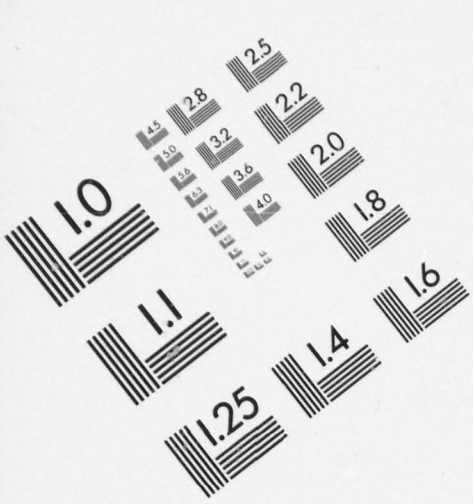
1/1

UNCLASSIFIED DEC 52 AEC-WT-515

F/G 19/11

NL

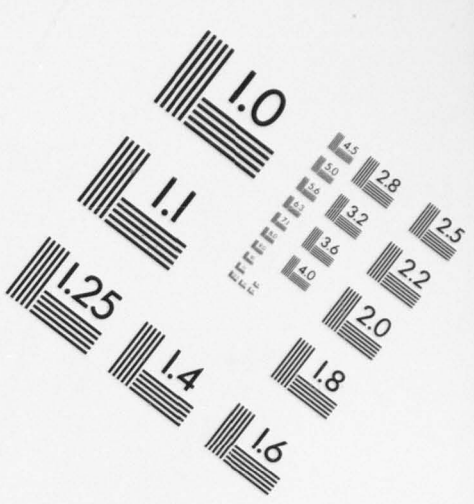




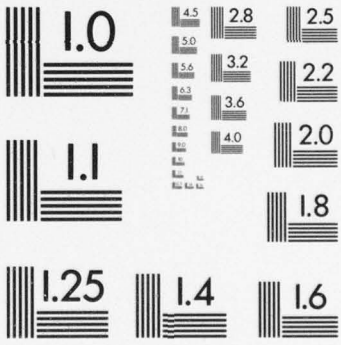
Association for Information and Image Management

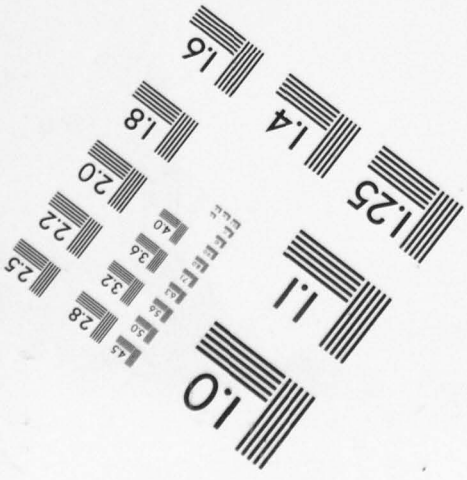
1100 Wayne Avenue, Suite 1100
Silver Spring, Maryland 20910

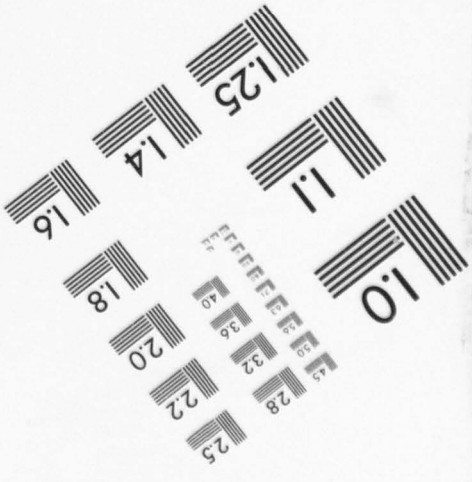
301/587-8202











MANUFACTURED TO AIIM STANDARDS
BY APPLIED IMAGE, INC.

UNCLASSIFIED



AD NUMBER

A078 547

NEW LIMITATION CHANGE

TO

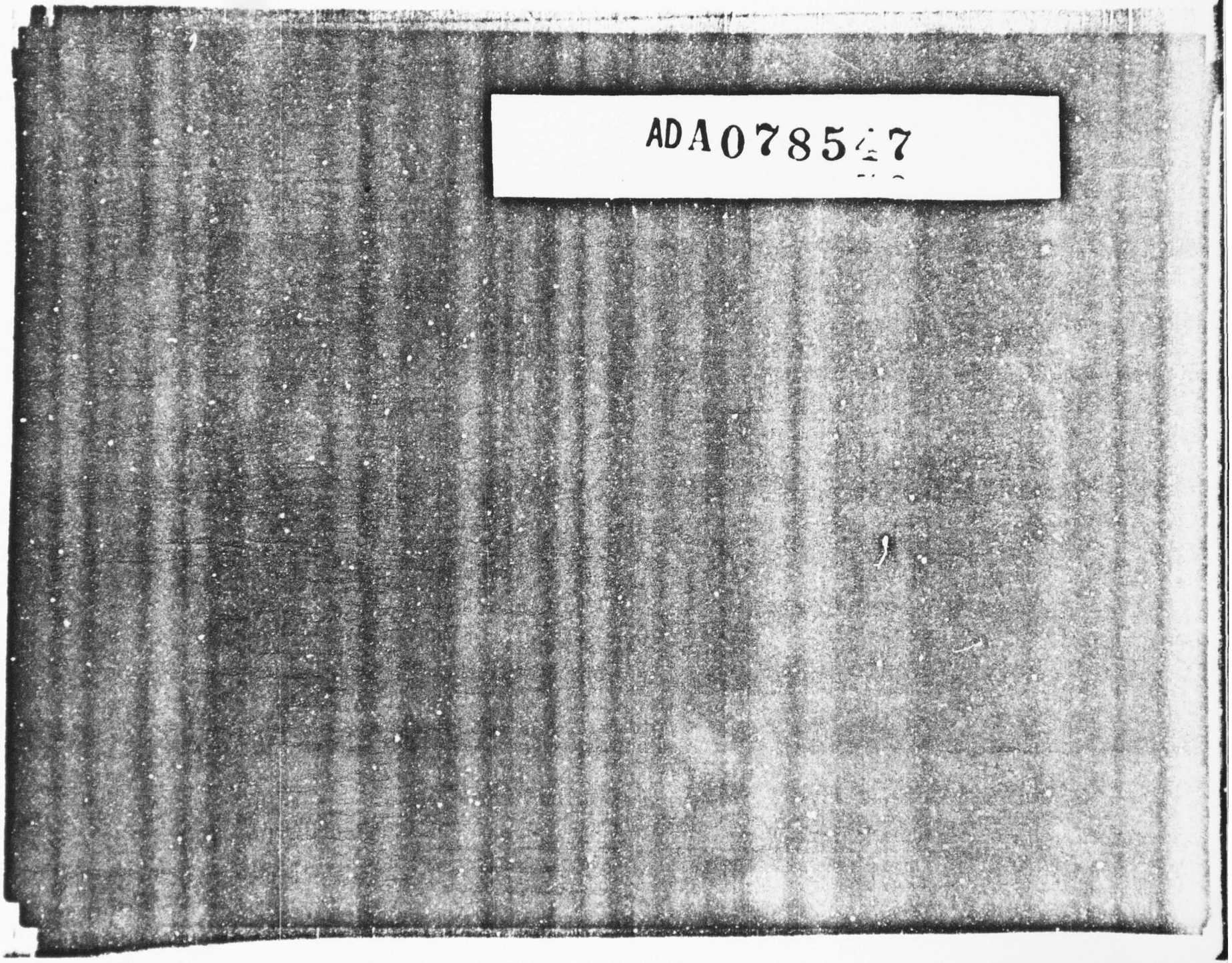
APPROVED FOR PUBLIC RELEASE DISRIBUTION U NLIMITED.

FROM

AUTHORITY

HQ DNA-IMTI LTR DTD 8 JUN 94

THIS PAGE IS UNCLASSIFIED


AD A078547

UNCLASSIFIED

This document consists of 1 page
221
Copy No. of 305 copies, Series A

U. S. ATOMIC ENERGY COMMISSION
TECHNICAL INFORMATION SERVICE
P. O. Box 401
Oak Ridge, Tennessee

Sept. 10, 1953

TO: Holders of Report WT-515

SUBJECT: ERRATA FOR REPORT WT-515

Changes as indicated in this notice were submitted after subject report had been printed and bound. It is requested that holders make the corrections as indicated below:

Page	Line	Should Read
3	13 from bottom	The blast efficiencies of Shots 1 and 2 were of the order of 62.7 per cent and 68 per cent respectively.
30	8 from bottom	On the basis of the value shown in Table 3.7 and Fig. 3.6, this efficiency for Shot 1 is 62.7 per cent.
52	3 from bottom	The blast efficiency determinations on Shots 1 and 2 indicated efficiencies of the order of 62.7 and 68 per cent respectively.

49 Table 3.7, Column 2, Slant Range (ft), R_s, should be changed as follows:

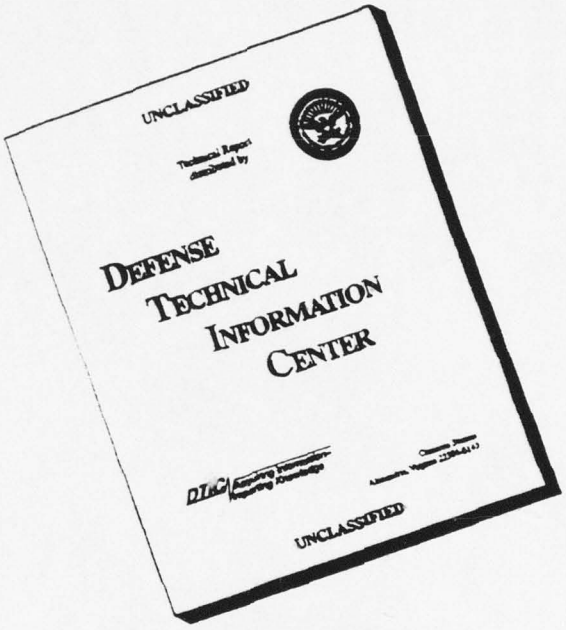
from 800	to 830
862	831
1110	1045
1039	1073
1508	1421
1987	1843

49 Table 3.7, Column 8, Blast Efficiencies, Shot 1, should be changed as follows:

from 69	to 74
75	63
75	62.5
76	64
73	61
69	57

RESTRICTED DATA
CONFIDENTIAL
SECURITY INFORMATION
UNCLASSIFIED

DISCLAIMER NOTICE



THIS DOCUMENT IS BEST QUALITY AVAILABLE. THE COPY FURNISHED TO DTIC CONTAINED A SIGNIFICANT NUMBER OF PAGES WHICH DO NOT REPRODUCE LEGIBLY.

UNCLASSIFIED

[redacted]

SECURITY INFORMATION

This document contains information affecting the national defense of the United States within the meaning of the Espionage Laws, Title 18 U. S. C., Sections 793 and 794. The transmission or the revelation of its contents in any manner to an unauthorized person is prohibited by law.

[redacted]

UNCLASSIFIED

UNCLASSIFIED

This document consists of 75 pages
No. 226 of 305 copies, Series A

OPERATION TUMBLER

Project 1.4

AIR BLAST MEASUREMENTS

REPORT TO THE TEST DIRECTOR

December 1952

Ballistic Research Laboratories
Aberdeen Proving Ground, Aberdeen Maryland

UNCLASSIFIED

Reproduced Direct from Manuscript Copy by
AEC Technical Information Service
Oak Ridge, Tennessee

Inquiries relative to this report may be made to

Chief, Armed Forces Special Weapons Project
P. O. Box 2610
Washington, D. C.

If this report is no longer needed, return to

AEC Technical Information Service
P. O. Box 400
Oak Ridge, Tennessee

UNCLASSIFIED

ABSTRACT

The objective of Project 1.4 was primarily to determine the general shape of that portion of a shock wave propagated near the ground but originating from an atomic explosion high in the air. Secondary objectives were the calculation of peak pressures involved and the computation of a blast efficiency for each bomb.

To achieve these purposes the shock arrival time method was used with blast switches at three levels above the ground both in the regular reflection and Mach reflection regions.

The air shock arrival times clearly indicated that the free air shock velocity was higher in the layer from 10 feet above the ground to ground level than it was in the layer between 50 feet and 10 feet above the ground. The increased velocity near the ground is probably due to a heated layer of air near the ground caused by radiation from the bomb. On Shot 4, the air shock arrival times corroborate the existence of a precursor shock as observed by other methods. In the Mach region the shock front appears to be vertical between the ground and 50 feet in the air. The pressures calculated for Shots 1 and 4 in the Mach region are in fair agreement with curves presented in Supplement 1 to the Capabilities of Atomic Weapons. The blast efficiencies of Shots 1 and 2 were of the order of 75 per cent and 68 per cent respectively. No blast efficiency was computed for Shot 4 due to the lack of free air data.

In the interests of economy and time spent in the field, a directional radio telemetric system for measuring blast arrival times was investigated. Approval was obtained to test the feasability of this method in conjunction with TUMBLER-SNAPPER Shot 6. Using pulse transmission and directive antenna system, information was obtained which substantiated the feasibility of such a method and points the way to successful design of compact and reliable components in the future. Peak air pressures can be determined from these arrival times by use of the Rankine-Hugoniot relations.

[redacted]

CLASSIFIED

CONTENTS

ABSTRACT 3

ILLUSTRATIONS. 7

TABLES 8

PART I AIR BLAST MEASUREMENTS BY A SHOCK ARRIVAL TIME METHOD. . . 9

CHAPTER 1 INTRODUCTION 11

1.1 Objective. 11
1.2 Methods. 11
1.3 History. 11
1.4 Basic Formulae 12
1.5 Corrections 14
1.6 Errors 16

CHAPTER 2 EXPERIMENTAL PROCEDURE 19

2.1 General 19
2.2 Field Layout 19
2.3 Instrumentation 19
2.3.1 Blast Switches and Mounts 20
2.3.2 Capacitor Banks 22
2.3.3 Cables. 22
2.3.4 Blast Hut Equipment 27
2.3.5 Playback Equipment. 32

CHAPTER 3 RESULTS AND DISCUSSION. 37

3.1 Primary Results. 37
3.2 Secondary Results. 37
3.2.1 Shot 1 37
3.2.2 Shot 2 41
3.2.3 Shot 4 47
3.2.4 Peak Pressures. 47
3.2.5 Blast Efficiencies 50

CHAPTER 4 CONCLUSIONS AND RECOMMENDATIONS 52

4.1 Conclusions. 52
4.2 Recommendations 53

[redacted]

CONTENTS (Cont'd)

PART II FEASIBILITY TEST OF RADIO TELEMETRIC SYSTEM FOR MEASURING AIR BLAST ARRIVAL TIMES ON AN ATOMIC DETONATION 55

CHAPTER 5 INTRODUCTION 57

5.1 Objective 57
5.2 General 57
5.3 Basic Plan 57

CHAPTER 6 INSTRUMENTATION 58

6.1 Overall System 58
6.1.1 Blast Switch 58
6.1.2 Transmitter 58
6.1.3 Receiver 60
6.1.4 Recording 62
6.1.5 Monitoring 62
6.1.6 Permanent Record 62
6.1.7 Blast Line Layout 62

CHAPTER 7 TEST RESULTS 64

7.1 Equipment Performance and Observations 64
7.1.1 Visual Monitoring 64
7.1.2 Recovery Party Observations 65
7.1.3 Playback Results 65

CHAPTER 8 CONCLUSIONS AND RECOMMENDATIONS 66

8.1 Conclusions 66
8.2 Recommendations 66

BIBLIOGRAPHY 68

ATOMIC ENERGY ACT 1946

UNCLASSIFIED
SECRET
Security Information

ILLUSTRATIONS

2.1 View of the Blast Line in the Frenchman Flat Area Looking Toward Ground Zero 20
2.2 Diagram of the Blast Line in the Frenchman Flat Area for TUMBLER 1 21
2.3 Diagram of the Blast Line in Area 7 for TUMBLER 2. 21
2.4 Diagram of the Blast Line in Area 7 for TUMBLER 4. 21
2.5 Schematic Diagram of a Blast Station Arrangement as Used on All Blast Lines 22
2.6 Block Diagram of the Air Shock Arrival Time Equipment 23
2.7 A Blast Switch Mounted in an Aluminum Casting. 24
2.8 Blast Switch Mount for the 10-foot and Ground Level Switches . 24
2.9 Blast Switch Mount for the 50-foot Level Switches 24
2.10 Schematic Diagram of a Three Channel Capacitor Bank as Used at Each Blast Station 25
2.11 Capacitor Bank and Buried Container as Used at Each Blast Station 26
2.12 Interior View of a Blast Hut 26
2.13 Block Diagram of a Single Data Channel of the Air Shock Arrival Time Equipment 28
2.14 Circuit Diagram of Two Channels of the Air Shock Arrival Time Equipment 29
2.15 Circuit Diagram of the Timing Oscillator and the Frequency Divider 30
2.16 Block Diagram of the Sequence Timer 31
2.17 Circuit Diagram of the Sequence Timer 33
2.18 Block Diagram of the Playback Recording System 34
3.1 Blast Arrival Times in Free Air. 39
3.2 Blast Arrival Times in Mach Region 40
3.3 Free Air Pressure vs Distance, Corrected to 1 KT at Sea Level. 46
3.4 Mach Pressure vs Distance, Corrected to 1 KT at Sea Level . . 46
3.5 Height of Burst Curves Corrected to 1 KT at Sea Level 48
3.6 Shots 1 and 2 in Free-Air Compared with Kirkwood-Brinkley Spherical Cast TNT Curve Scaled to 1 KT. 48
3.7 Configuration of Effective Sub-base Length in Free Air 51
6.1 Aluminum Foil Switch 59
6.2 Basic Components of Foil Switch. 59
6.3 Beacon Transmitter 61
6.4 Pulse Processing Circuit 63

[redacted] [redacted]
UNCLASSIFIED

UNCLASSIFIED

TABLES

3.1 Time of Shock Arrival 38

3.2 Air Temperatures from Velocity Measurements 41

3.3 Peak Pressures from Time of Shock Arrival - Shot 1. 42

3.4 Peak Pressures from Time of Shock Arrival - Shot 2. 43

3.5 Peak Pressures from Time of Shock Arrival - Shot 4. 44

3.6 Test Conditions 45

3.7 Blast Efficiencies. 49

UNCLASSIFIED

UNCLASSIFIED

PART I

AIR BLAST MEASUREMENTS BY A SHOCK ARRIVAL TIME METHOD

BY

MARVIN F. CLARKE and ROBERT A. EBERHARD

ACKNOWLEDGMENTS

The preparation necessary to the success of a field program of the magnitude of Project 1.4 was no small task. Its successful conclusion was due to the cooperation and the unstinted efforts of many people.

Acknowledgement is hereby made of the aid given by the members of the field group as listed below:

Edward J. Bryant	Installation
Marvin F. Clarke	Supervisor
Robert A. Eberhard	Data Reduction
Gerald F. Ginty	Instrumentation
Robert P. Long	Supply
William T. Matthews	Installation
Julius J. Meszaros	Liaison
John W. Mobarry	Instrumentation
William J. Taylor	Installation

Acknowledgement is made of the aid given by the personnel of the Explosion Kinetics Branch of the Terminal Ballistics Laboratory in preparation of the equipment with special thanks to James I. Randall and George A. Coulter.

The initial planning and overall supervision were carried out by Dr. C. W. Lampson, Chief, Terminal Ballistics Laboratory, Dr. E. E. Minor, Project Director, and his deputy, Mr. Wesley E. Curtis.

UNCLASSIFIED

UNCLASSIFIED

CHAPTER 1

INTRODUCTION

1.1 OBJECTIVES

The primary purpose of Project 1.4 was to determine the general shape of that portion of the shock wave propagated near the ground but originating from an atomic explosion high in the air.

The secondary objectives were to calculate the peak pressure versus distance relationship in the regions of regular and Mach reflection of the shock wave and to compute a blast efficiency for each bomb.

1.2 METHODS

To achieve the primary objectives stated above, a method was adopted for measuring the air shock arrival time at several heights above the ground and at several points along a line radiating from ground zero which is directly below the point of detonation of the bomb. This method required two primary measurements - the distances from the point of detonation of the bomb to the blast switches and the time durations between the detonation and the arrival of the shock wave at the blast switches.

To achieve the secondary objectives stated above, one must also measure the ambient conditions of the air mass through which the shock wave was propagated and assume that the Rankine-Hugoniot relationship between the peak pressure of the shock front and the velocity of propagation of the shock front was applicable.

1.3 HISTORY

The air shock arrival time method of measuring blast waves had been used with fair success on Operations SANDSTONE, GREENHOUSE, and JANGLE. This method involved only the variables length and time, both of which can be measured accurately for tests on large explosions. The simplicity with which the measurements could be made and the reliability of the system were its chief advantages.

The shock wave from small charges detonated near a reflecting surface such as the ground was known to have a sharp rise to peak pressure both in the regular reflection region and in the region of Mach reflection.

UNCLASSIFIED

Measurements made near the ground on atomic explosions on Operation GREENHOUSE (shots Dog and Easy) indicated some peculiar wave shapes in the region of Mach reflection. On Operation BUSTER, the shock pressures measured near the ground were found to be considerably lower than those predicted from previous shots. The shape of the blast wave in the high pressure region near the ground was such that a comparatively long time was required for the shock wave to reach a peak pressure.

One explanation for part of these apparent discrepancies was based on the tremendous amount of heat radiated from an atomic explosion. It was thought that the heating of the ground by radiation might cause a layer of heated air near the ground which would have a significant effect on the shape and the rate of propagation of the shock front. Knowledge of the shape of the shock front in and around this heated layer of air would shed some light on these phenomena. By the nature of the shock arrival time measurements, it was believed that the distortion of the shock front in the region close to the ground could be discerned. It is evident that extreme care must be exercised in evaluating arrival time data in terms of peak pressures in the regions affected by such phenomena.

1.4 BASIC FORMULAE

The air shock arrival time data permits the determination of the average shock velocity between any two successive blast switches. The computations of average velocity were carried out only in the regions where an ideal shock front was substantiated by the pressure-time data taken by other projects. The average velocity was obtained between any two successive stations (1 and 2) at the same height above the ground in the usual manner:

$$U = \frac{R_1 - R_2}{t_1 - t_2} \qquad (1.1)$$

where

R is the slant range from the burst to the blast switch if both stations are in the regular reflection region

or R is the ground range from the ground point directly beneath the burst to the blast switch if both stations are in the Mach reflection region

t is the total time duration from the instant of detonation to the arrival of the shock wave at the blast switch.

CLASSIFIED

The excess pressure of the shock wave over ambient barometric pressure is then calculated using the Rankine-Hugoniot relation for an ideal gas:

$$\frac{P_s}{P_o} = \frac{2\gamma}{\gamma+1}\left[\frac{U^2}{a_o^2} - 1\right] \qquad (1.2)$$

where

γ is the ratio of specific heats (1.4 for air)

U is the average shock velocity

P_s is the peak excess pressure of the shock wave above ambient barometric pressure

P_o is the ambient barometric pressure of the air into which the shock is advancing

a_o is the sound velocity in the air into which the shock wave is advancing

A major step necessary in this computation was to substitute the sound velocity in the air into which the shock wave was advancing after the ambient temperature of the air was known. The relationship between the sound velocity and the temperature may be stated

$$a_o = 1088 \left(1 + \frac{T}{273}\right)^{1/2} \qquad (1.3)$$

where

T is the temperature in degrees Centigrade

For the purpose of these tests, the temperature was measured along the blast line near ground level before the detonation of the bomb.

If Equations (1.2) and (1.3) are combined, and solved for T, the following relationship is found:

CLASSIFIED

UNCLASSIFIED

$$T + 273 = \frac{U^2}{3720\, P_s/P_o + 4340} \qquad (1.4)$$

This relationship would permit the determination of the average temperature along a sub-base. The application of this relationship is subject to errors in the pressure approximations as well as the errors in the velocity determinations but the temperatures so obtained are thought to be fair approximations.

In order to compute average shock velocities, it is necessary to know whether the blast switches are located in the free air region, or in the region of Mach reflection. If the sub-base is in the free air region, then the sub-base length is the difference in the slant ranges to the two blast switches. If the sub-base is in the region of Mach reflection, then the sub-base length is the difference in the ground ranges to the two blast switches. If a sub-base has one blast switch in the free air region and one blast switch in the region of Mach reflection, then it is not usable for either determination.

The blast efficiencies in terms of T.N.T. were obtained in the following manner. Figure 3.5 shows free air pressure versus distance, corrected to 1 LT at sea level, for shots 1 and 2. In Fig. 3.6 the Kirkwood-Brinkley theoretical curve for T.N.T. shows pressure versus distance, corrected to 1 LT. At a given measured pressure, a value for distance (R_1) is obtained from Fig. 3.5 and a value for distance (R_2) from the Kirkwood-Brinkley curve in Fig. 3.6. The blast efficiency of the bomb at this pressure level in terms of T.N.T. is found by the equation

$$E = (R_1/R_2)^3 \qquad (1.5)$$

For comparison purposes, the free air curves of Shots 1 and 2 have been fitted by eye and plotted in Fig. 3.6.

1.5 CORRECTIONS

The Rankine-Hugoniot relation is determined for a shock wave moving through a medium which is at rest. Since there is nearly always some motion of the air in the open, the shock velocity obtained by direct measurement of distance and time must be corrected to allow for the motion of the medium through which the shock was travelling. Corrections of the average velocity of the shock wave were made for wind components parallel to the direction of propagation of the shock wave

AT [redacted]

for those shots where a wind velocity of more than five miles per hour was reported.

The velocity of sound is affected by the amount of water vapor present in the air through which it is propagated.[3] The correction factor for the worst possible case in this series of shots was so small as to be negligible compared to the over-all accuracy of the data; therefore, humidity corrections were not made.

The method of correcting the velocity of sound for the temperature of the air through which it was propagated was shown in Equation 1.3.

The shock velocity determined experimentally is an average value over the interval between the blast switches used to record the time of arrival of the shock. In order to determine the distance at which the pressure calculated from Equation 1.2 is to apply, it is necessary to find the distance from the explosion at which this average velocity is equal to the instantaneous shock velocity. The equation for determining this distance may be stated as follows:

$$R_v = R_m \left[1 - \frac{(n+1)}{24} q^2 \right] \qquad (1.6)$$

R_v is the distance from the point of detonation to the point at which the average velocity equaled the instantaneous velocity

R_m is the distance from the point of detonation to the mid-point of the sub-base

q is the ratio of L/R_m, where L is the sub-base length

$-n$ is the slope of the pressure-distance curve assuming that the pressures occurred at the mid-points of the sub-bases as a first approximation

This equation applied for pressures (P_2) less than 17 pounds per square inch and for values of (q) less than two [3].

The elevations of the test sites for these tests were approximately 4000 feet above sea level. For comparison with previous tests, the pressure-distance curves were reduced to sea level and 1 KT by the following equations[4]

[redacted] [redacted]

UNCLASSIFIED

$$P_s(\text{sea level}) = P_s(\text{test site}) \times \frac{P_o(\text{sea level})}{P_o(\text{test site})} \tag{1.7}$$

$$R_v(\text{sea level}) = R_v(\text{test site}) \left[\frac{P_o(\text{test site})}{P_o(\text{sea level}) \times w}\right]^{1/3} \tag{1.8}$$

$$H_b(\text{sea level}) = H_b(\text{test site}) \left[\frac{P_o(\text{test site})}{P_o(\text{sea level}) \times w}\right]^{1/3} \tag{1.9}$$

w is the weight of the explosive in kilotons of TNT as computed from the Radiochemical yield.

1.6 ERRORS

The contribution of errors in the measurements of distances, times and temperatures to the error in the computed peak pressure of the shock wave is given by the relation[15]:

$$\frac{\Delta P_s}{P_s} = 2\left[1 + \frac{7 P_o}{6 P_s}\right]\left[\frac{\Delta s}{s} - \frac{\Delta t}{t} - \frac{\Delta a_o}{a_o}\right] \tag{1.10}$$

s is the effective sub-base length

t is the time duration between the shock arrivals at successive blast switches

a_o is the velocity of sound in the undistrubed air ahead of the shock wave.

The error in the computed velocity of sound due to an error in the measurement of the temperature of the air through which the sound was propagated may be stated:

$$\frac{\Delta a_o}{a_o} = \frac{\Delta T}{2T} \tag{1.11}$$

where T is the absolute temperature (Kelvin).

[redacted]

If this value of $\frac{\Delta a_o}{a_o}$ is inserted in Equation 1.9 the sum of the absolute values of the maximum fractional error in each measurement of distance, time and temperature, may be used to determine the maximum fractional error in the peak pressures which were computed. Over the range of pressures covered in this report, the fractional error in the peak pressures computed would be 4 to 14 times the sum of the absolute values of the fractional errors in distance, time and temperature measurements.

The maximum possible error in the location of the point of detonation of the bomb could cause an error of ±4 feet in the effective sub-base lengths. For those sub-bases near ground zero on Shots 1 and 2, this would account for an error of ±15 per cent in the peak pressures computed. Other errors due to measurements between stations and sub-base calculations are assumed negligible.

The maximum possible error in the determination of time between the arrival of the shock wave at two successive stations was 1 millisecond. This error is always positive since it is due to delay in closure of the blast switches.

The determination of the temperature of the air through which the shock wave was advancing can only be approximated within wide limits. Air temperature measurements along the blast line indicate considerable heating of the air near the ground due to radiation from the bomb prior to the arrival of the shock wave. There is insufficient data available to even estimate what variations in air temperature may have existed along the effective sub-bases for the various shots. An increase of air temperature of 5 degrees centigrade would lower the pressures reported here 3 to 12 per cent.

On the basis of these possible errors in time, distance, and temperature, the peak pressures computed from the shock arrival time data are good to ±20 per cent.

The configuration of the blast line with respect to the point of detonation of the bomb was such that the portion of the shock front which activated each blast switch was different and had traversed a different path from the bomb to the blast switch. Thus, small irregularities in the sphericity of the shock front or in the homogeneity of the air mass through which the shock front was advancing become important. Yet both factors are almost impossible to evaluate.

[redacted]

The limitation on the length of the effective sub-bases and the low pressure levels near ground zero, meant that the inherent inaccuracy was largest there. The location of the blast switches in the layer of air where temperature variations due to thermal radiation existed was also a source of error which is magnified by the low pressures encountered. These difficulties were forseen, but since the arrival time data was available it was thought worthwhile to compute peak pressures for comparison with the other systems in spite of the probable errors.

UNCLASSIFIED

CHAPTER 2

EXPERIMENTAL PROCEDURE

2.1 DETAIL

The instrumentation necessary to make the air shock arrival time measurements desired for Operation TUMBLER was obtained only after numerous compromises. The short time allowed for the preparation of the equipment before the tests necessitated the use of equipment previously used for Operation JANGLE. Since only part of the equipment was useable, the number of stations which could be installed was limited. To reduce the amount of wire required, it was decided to use a parallel network along the blast line. This meant that the system used on previous tests had to be extensively revised to insure that data could be obtained on a network during the time that an atomic explosion was in process at the other end of the wire.

The geometric relationship between the point of detonation of the bomb and the blast line limited the high pressure range which could be covered. The response time of the blast switches limited the low pressure range which could be covered.

2.2 BLAST LINES

A view of the blast line in the Frenchman Flat Area looking toward ground zero is shown in Fig. 2.1. The picture shows part of the scaffolding being removed from one of the instrument towers just prior to shot time. The blast switch mounted at the 50-foot level was located near the top of the tower on the right in the picture. The blast switches mounted at the 10-foot level and at ground level were located on the short pole approximately 15 feet to the right of the right tower. A diagram of the blast line in the Frenchman Flat Area is shown in Fig. 2.2. Diagrams of the blast lines in Area 7 are shown in Fig. 2.3 and 2.4. A diagram of a blast station layout as used on all blast lines is shown in Fig. 2.5.

2.3 RECORDING STATION

Air shock arrival times were obtained by blast switch closures when the air shock arrived at each station. When a switch closed, it discharged a capacitor initiating a signal which was transmitted by

UNCLASSIFIED

UNCLASSIFIED

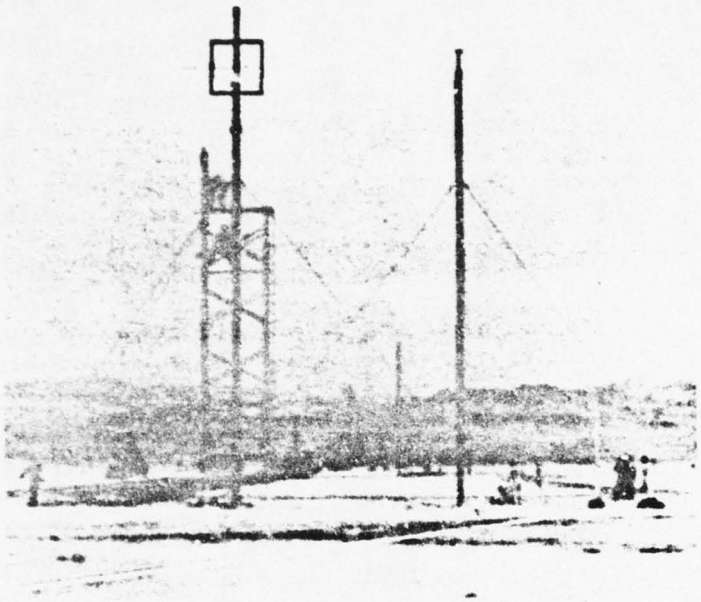


Fig. 2.1 View of the Blast Line in the Frenchman Flat Area Looking Toward Ground Zero

cable to the blast hut. At the blast hut, the signal was superimposed on a 10 kc timing signal and recorded on a magnetic tape recorder. A photo-tube gave a zero time signal initiated by the flash of the explosion. A block diagram of the instrumentation is shown in Fig. 2.6.

2.3.1 Blast Switches and Mounts

Two types of blast switches were used. Both were made by General Electric, but one was glass, the FA-15, and the other was metal-cased, the FA-6. Slight differences in the manner of bringing out the leads also existed. The switch contacts were in an evacuated tube to reduce leakage when the contacts are irradiated. The moving element of the switch was a long tubular arm pivoted on a flexible diaphragm which sealed one end of the vacuum tube. A circular paddle was fixed to the exposed end of this arm for the shock wave to strike. A small magnet was used to hold the switch in the open position until the shock wave arrived.

Two types of mounting were used for these blast switches. The 10-foot and ground level switches were mounted in aluminum castings as shown in Fig. 2.7 and 2.8. The 50-foot level switches were mounted as shown in Fig. 2.9.

UNCLASSIFIED

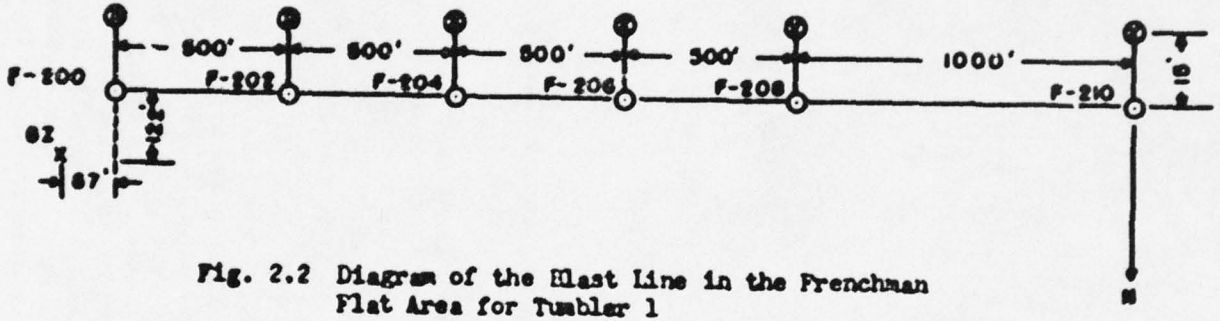


Fig. 2.2 Diagram of the Blast Line in the Frenchman Flat Area for Tumbler 1

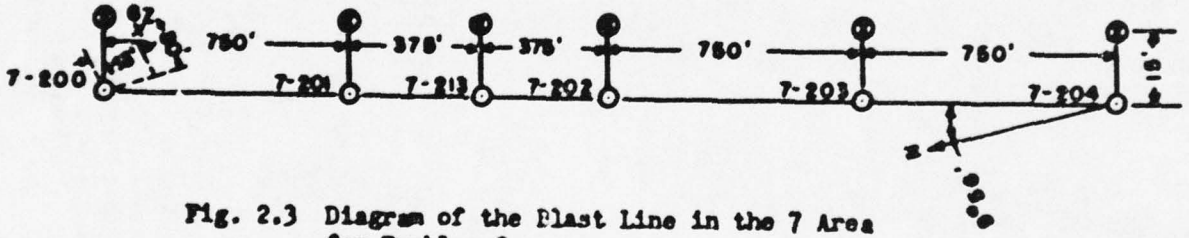


Fig. 2.3 Diagram of the Blast Line in the 7 Area for Tumbler 2

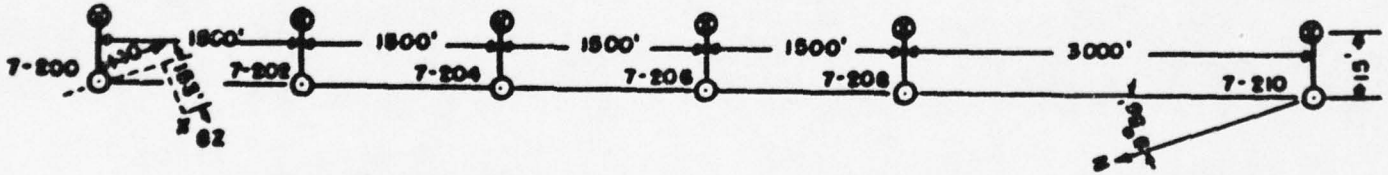


Fig. 2.4 Diagram of the Blast Line in the 7-Area for Tumbler 4

LEGEND:
⊙ 50 FT. GAGE HEIGHT
⊕ 0 FT. AND 10 FT. GAGE HEIGHT

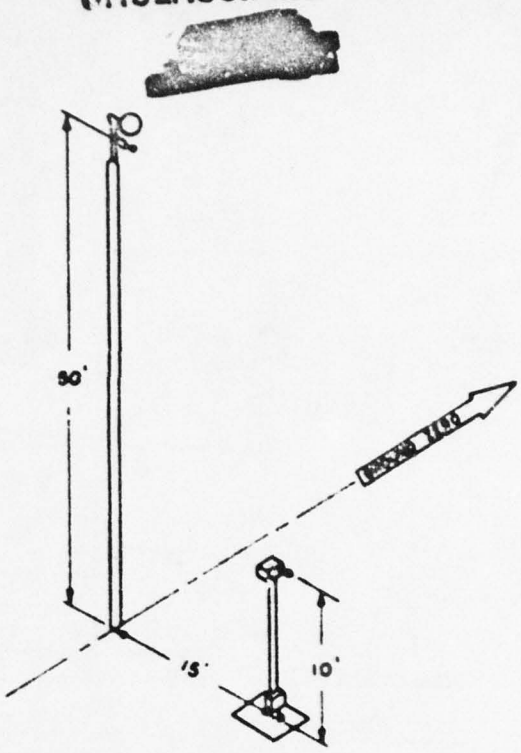


Fig. 2.5 Schematic Diagram of a Blast Station Arrangement as Used on All Blast Lines

2.3.2 Capacitor Banks

The blast switches were connected in such a manner that the switch closure aborted a charged capacitor to initiate a signal for transmission to the blast hut. A schematic diagram of a capacitor bank showing three channels, one for each gage height at a particular station is shown in Fig. 2.10. A 1/16 ampere fuse was connected in series with each blast switch so that only the first shock arrival at each switch would be recorded. The capacitor discharge across this fuse caused the fuse to blow thus opening the circuit so that any subsequent closure of the blast switch would not be recorded. This capacitor was not charged until 30 seconds before the detonation of the bomb to reduce the possibility of blowing the fuse due to wind closing the switch. The capacitor bank and its buried container may be seen in Fig. 2.8 and 2.11.

2.3.3 Cables

All of the blast switches mounted at a single height above the ground along the blast line were connected in parallel across a single cable. Three cables were used for each blast line. A fourth cable was laid in the ditch along the blast line to be used in the event any wire trouble developed after the ditches were closed. This

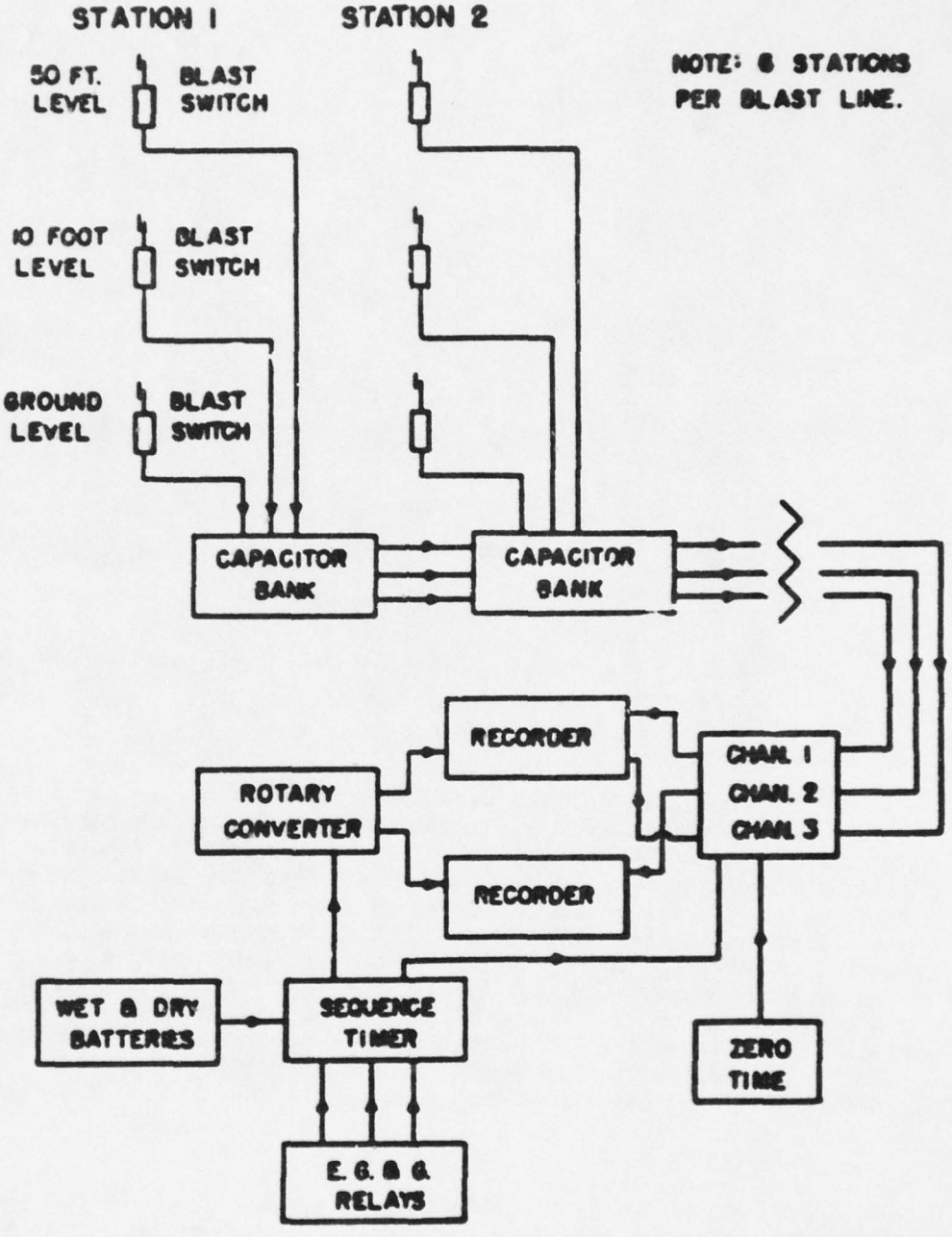


Fig. 2.6 Block Diagram of the Air Shock Arrival Time Equipment

UNCLASSIFIED

Fig. 2.7 A Blast Switch Mounted in an Aluminum Casting

Fig. 2.8 Blast Switch Mount for the 10 ft. and Ground Level Switches. The Extra Switch at the 10 ft. Level was an Experimental Addition.

Fig. 2.9 Blast Switch Mounts for the 50 ft. Level Blast Switches

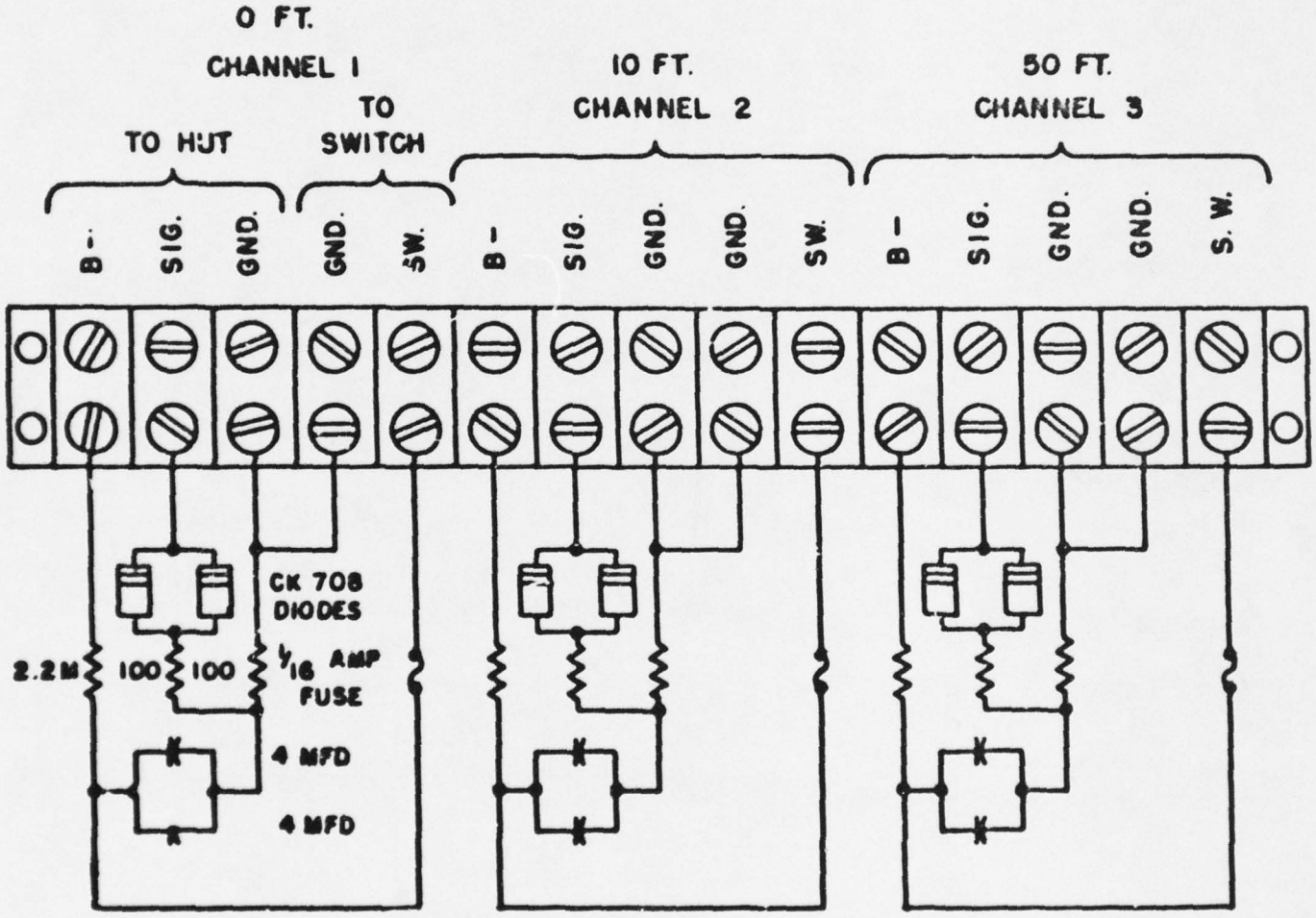


Fig. 2.10 Schematic Diagram of a 3-Channel Capacitor Bank as Used at Each Blast Station

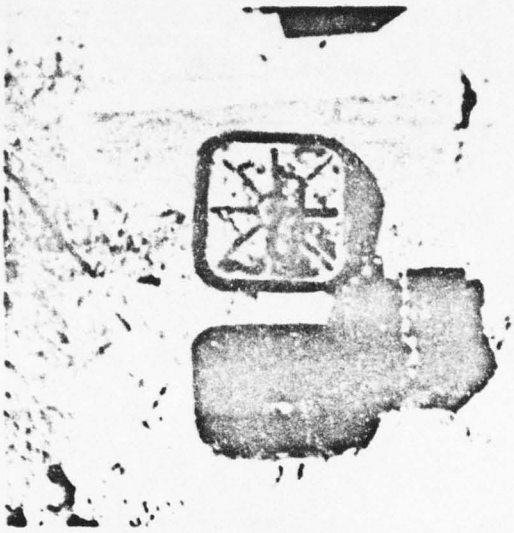


Fig. 2.11 Capacitor Bank and Buried Container as Used at Each Blast Station

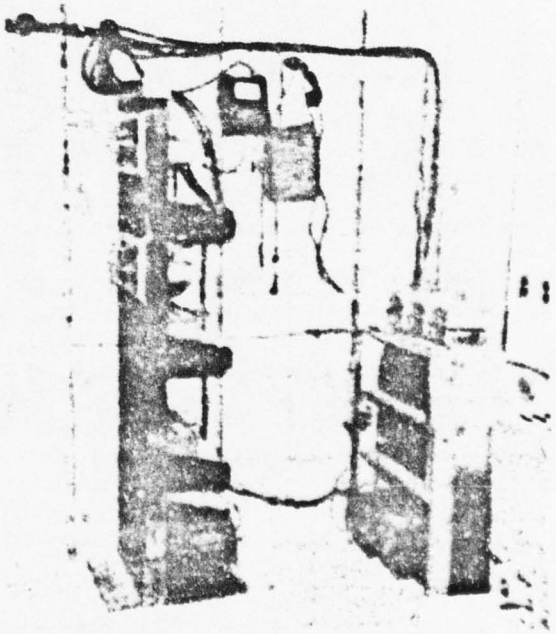


Fig. 2.12 Interior View of a Blast Hut Showing the Air Shock Arrival Time Equipment

UNCLASSIFIED

cable was used for telephone communications between the blast hut and the blast stations during check-out of the instrumentation.

The cable was manufactured by the Belden Manufacturing Company and was Type 8C06-2, two conductor, shielded, rubber-covered cable. As employed in this test, the cable was used as a three conductor cable with the shield serving as a ground return line. All grounds were made at the blast hut to prevent ground loops which might have varying potentials at the time of the shot. The cable was brought out of the blast switches through the center of the iron pipes which supported the blast switch mounts to a ditch in the ground. All cables were buried approximately 18 inches deep between the blast stations and the blast hut.

2.3.4 Blast Hut Equipment

The arrangement of the equipment located in the blast hut is shown in Fig 2.12. Only one relay rack was required for the instruments plus a shelf for the wet and dry batteries and the Edgerton, Germeshausen & Grier (EG&G) relays. The blast hut in the Frenchman Flat Area had an adequate floor space of 6 by 6 feet.

A block diagram of a single data channel is shown in Fig. 2.13. Three such channels were provided, one for each gage along the blast line. A circuit diagram of the air shock time equipment is shown in Fig. 2.14. This diagram includes the recording channels with their timing signal oscillator, zero time pulse input circuits, mixer circuits, and associated connections. Two such circuits were incorporated on a single chassis thus providing four data channels with two independent timing oscillators.

The 10 kc timing oscillators were crystal-controlled to insure accuracy of timing. A circuit diagram of the 10 kc oscillator and the frequency divider used to provide 100-cycle markers on the records is shown in Fig. 2.15. The frequency of this oscillator was checked against WWV as a standard frequency and was found to be constant to approximately on part in 200,000 under the conditions imposed by these tests. The frequency divider consists of two stages of 10 to one division achieved by means of synchronized astable multivibrators. When properly adjusted, synchronization is retained for variations of plus or minus 5 per cent in the natural period of the multivibrators.

A zero time pulse was initiated when the flash of the explosion reached a photo-tube. The photo-tube and its associated circuit was provided in a Blue Box furnished by EG&G. Optical filters

UNCLASSIFIED

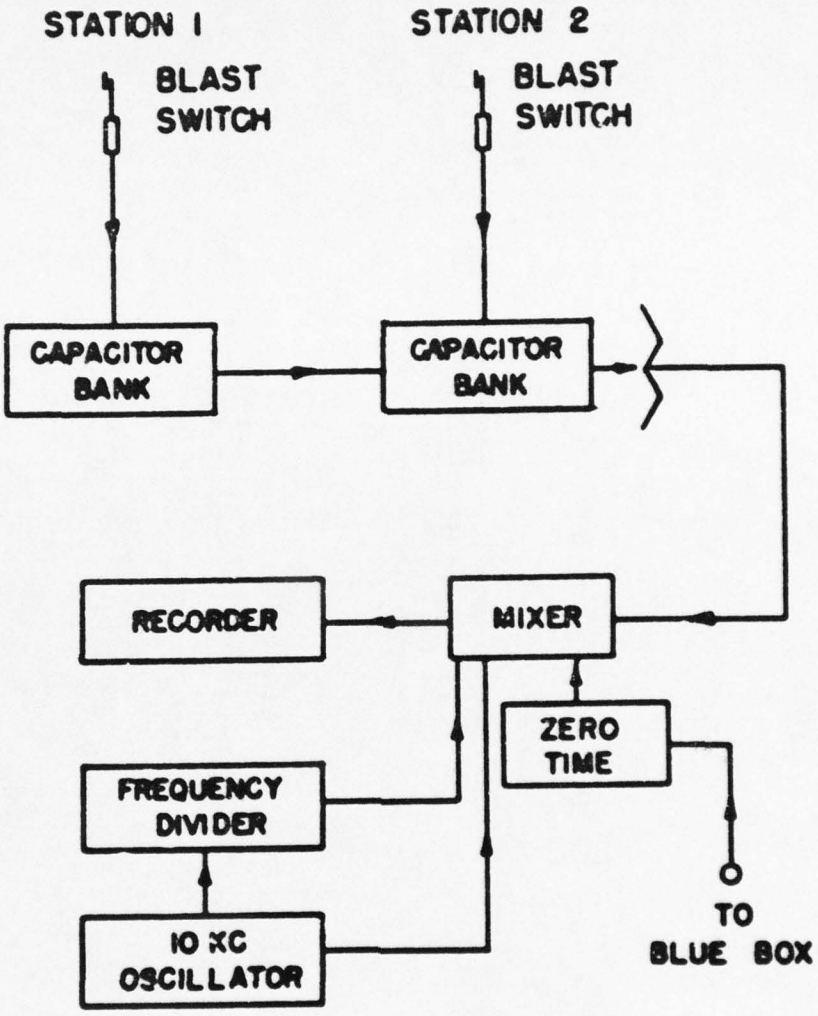


Fig. 2.13 Block Diagram of a Single Data Channel of the Air Shock Arrival Time Equipment

UNCLASSIFIED

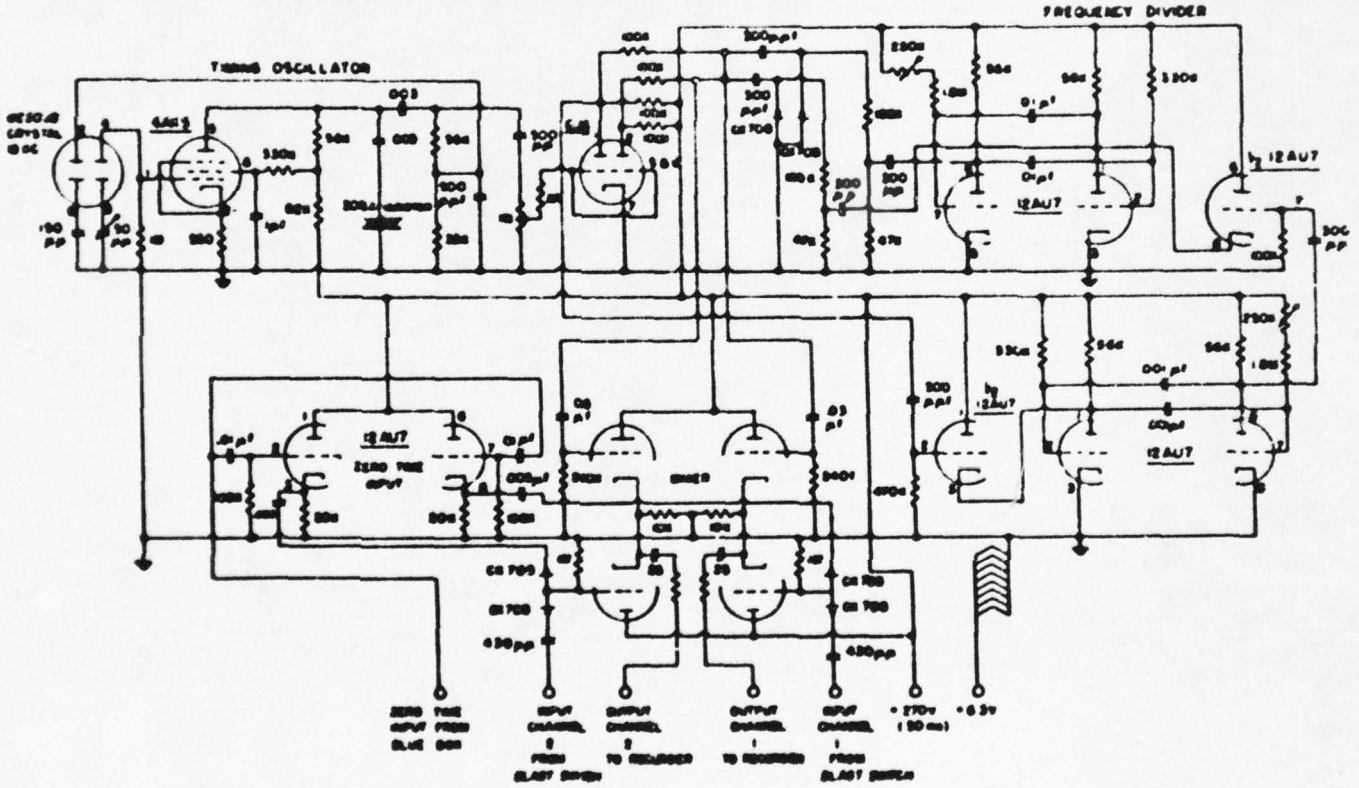


Fig. 2.14 Circuit Diagram of Two Channels of the Air Shock Arrival Time Equipment

UNCLASSIFIED

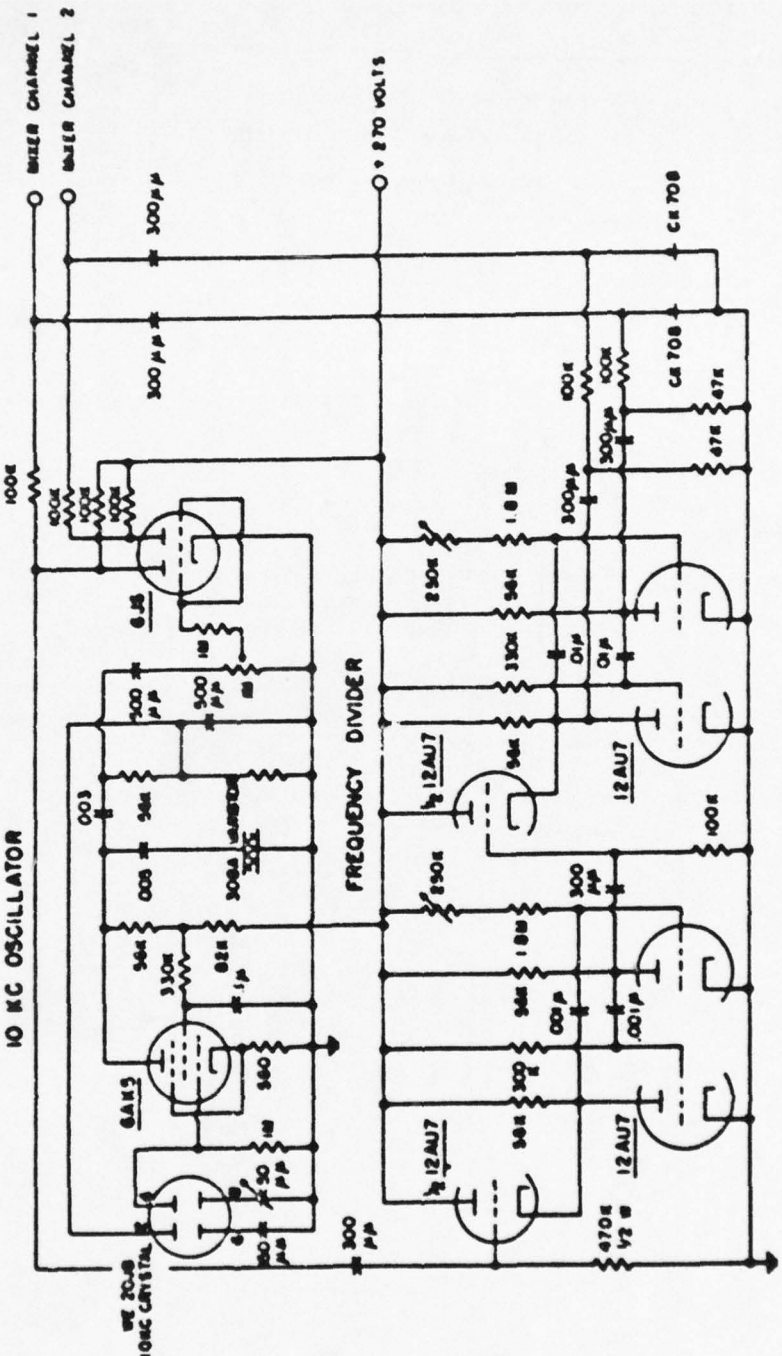


Fig. 2.15 Circuit Diagram of the Timing Oscillator and the Frequency Divider

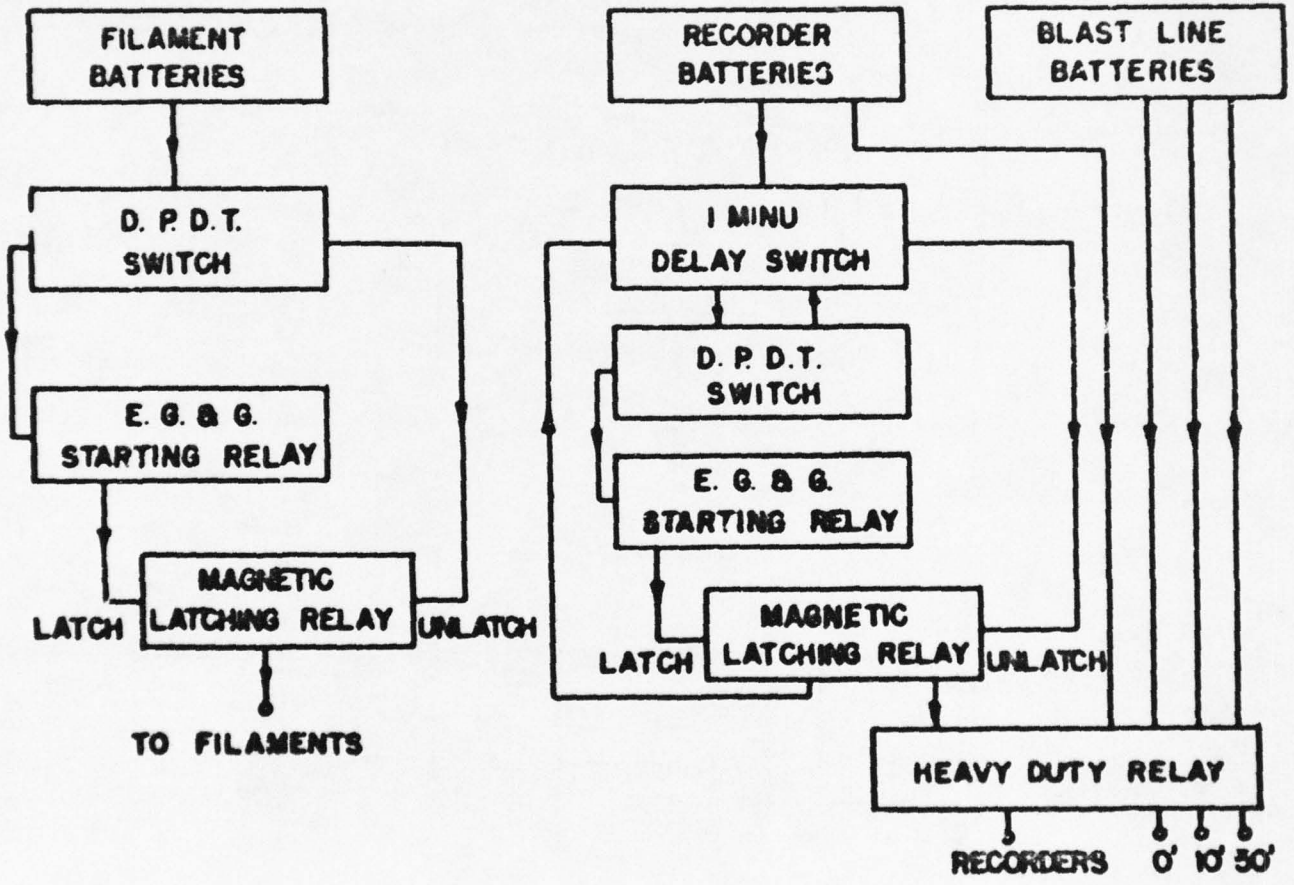


Fig. 2.16 Block Diagram of the Sequence Timer

were also provided to prevent premature triggering of the zero time pulse by sun light or other optical disturbances.

The shock arrival signals from the blast switches, the zero time pulse, and the 10 kc timing signals were all combined in the cathode circuit of a mixer tube which was connected to a tape recorder.

The tape recorders used on this test were Magnacorders, Type PT6AH, made by Magnacord, Inc. They were two channel recorders using one-quarter inch wide magnetic tape. These particular recorders were further modified to eliminate the bias oscillator and to provide a solenoid operated cut-off switch to stop the recorder when the end of the recording tape was reached.

A sequence timer was provided to start the various components at the proper times after it was activated by the EG&G timing signals. A minus 15 minute signal was used to start the warm-up period for the equipment and a minus 30 second signal was used to start the recorders and to supply charging voltages to the capacitor banks on the blast line. The sequence timer provided a 1 minute delay relay to stop the recorders and de-energize the equipment at plus 30 seconds. A block diagram of the sequence timer is shown in Fig. 2.16. A circuit diagram is shown in Fig. 2.17.

Power for operation of the air shock arrival time equipment was supplied from batteries. Wet cell batteries were used for the filament power supplies and to drive the rotary converters which ran the tape recorders. Dry cell batteries were used for all other power required except for the Blue Box. Since this equipment would have served its purpose before the shock wave reached it, the 110-volt ac power in the blast hut was used for its operation.

2.3.5 Playback Equipment

The air shock arrival time records were played back on the same type of recorder as the one on which the record was made. A single channel was played back at a time through a pre-amplifier to an oscilloscope. An oscillographic recording camera was used to make a permanent visible record of the data. A block diagram of the playback recording system is shown in Fig. 2.18.

The pre-amplifier used was a General Electric Vacuum Tube Voltmeter, Type AA-1. The pre-amplified signal was put into the Y-axis input of a DuMont Oscilloscope, Type 304H. The Y-axis amplifier of the oscilloscope was connected to the X-axis plates of the cathode ray tube. The sweep circuit was turned off. This resulted in a horizontal

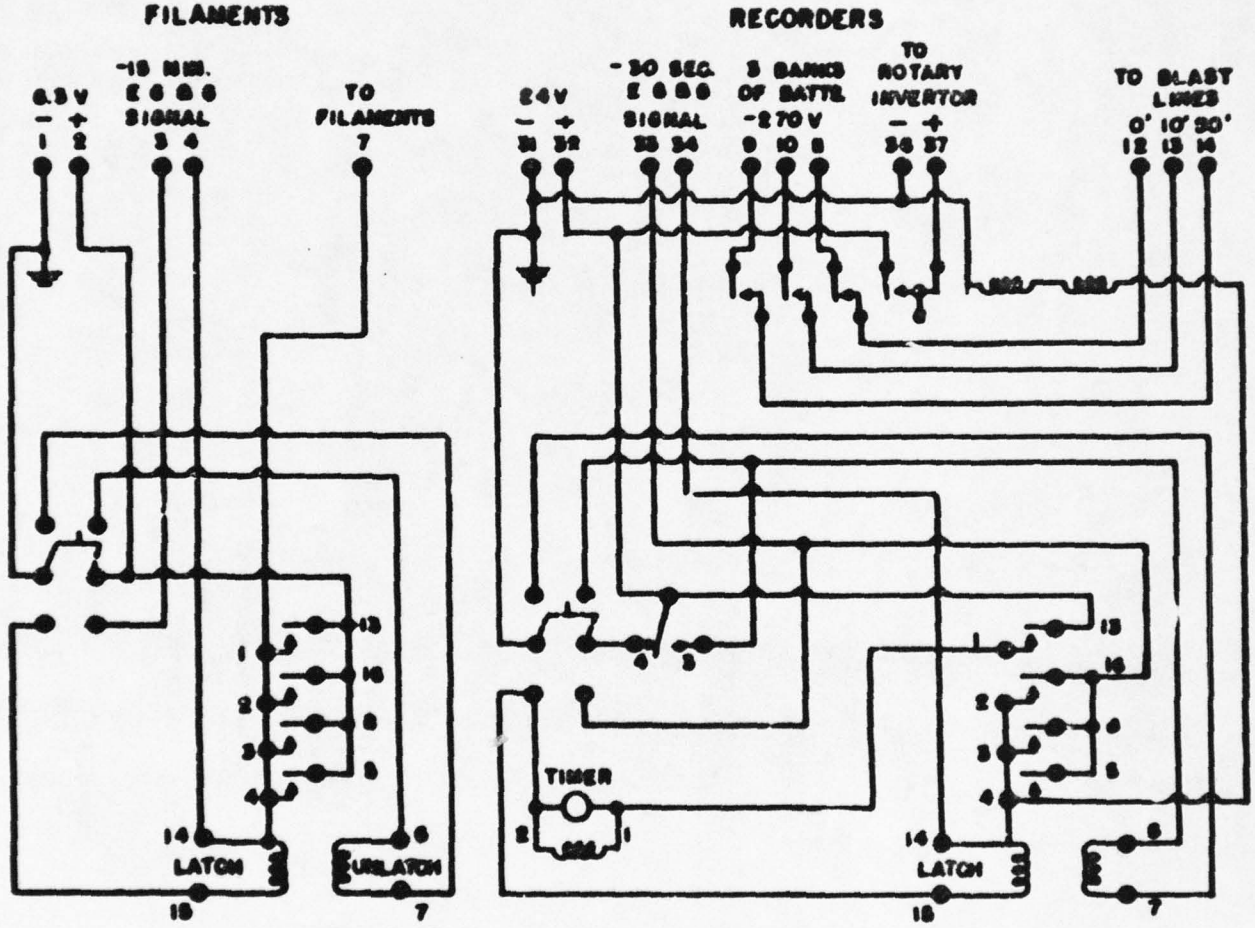


Fig. 2.17 Circuit Diagram of the Sequence Timer

UNCLASSIFIED

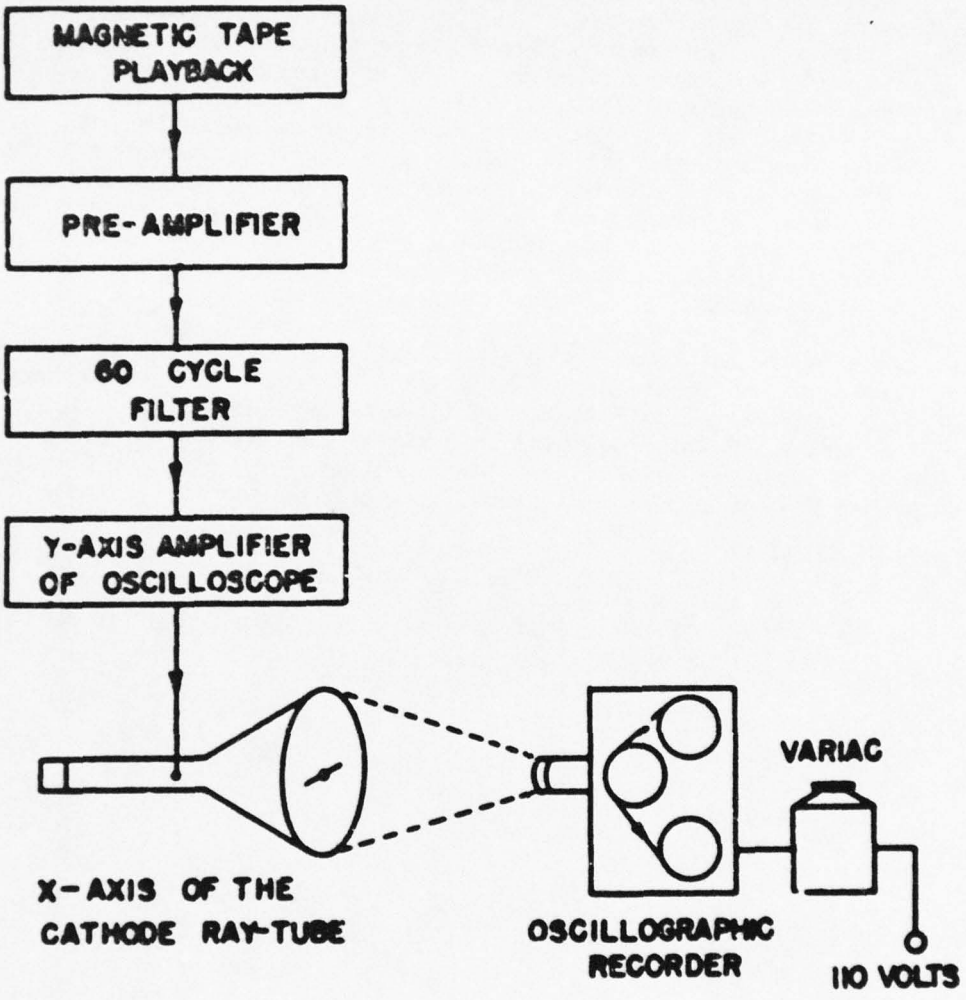


Fig. 2.18 Block Diagram of the Playback Recording System

excursion of the light beam proportional to the signal strength of the record being played back.

A General Radio Oscillographic Recorder Camera, Type 251Ae, was used to record the excursions of the light beam. Since this type of camera has no shutter and the film moves continuously past the lens in a vertical plane, the resulting record is a continuous 10 kc frequency wave drawn down the center of the 35mm film. The air shock arrival time pulse from each blast switch and the zero time pulse from the photo-tube were superimposed on the timing wave. The frequency divider also imposed a sharp pulse on the record for each hundredth cycle of the 10 kc wave. A Variac was used to control the voltage to the drive motor of the camera and this provided speed control for the recording film. Photographic developing equipment was provided to handle 100-foot lengths of 35mm film. Kodak Linagraph Pan film was used.

An illuminated viewing screen equipped with film rewinding equipment was used for preliminary examination of the records. Final count of the records to determine the time interval between the explosion and the arrival of the shock wave at a given blast switch was made by means of an enlarged view of the 35mm film record projected by a Kodagraph Film Reader, Type MPE, made by Eastman Kodak Company.

CHAPTER 3

RESULTS AND DISCUSSION

3.1 PRIMARY RESULTS

The primary data obtained on these tests by Project 1.4 were the air shock arrival times at known points along the ground. Table 3.1 lists these arrival times for Shots 1, 2, and 4 with the slant ranges and the ground ranges to each station. For data obtained in the free-air region, the air shock arrival times are plotted versus slant range in Fig. 3.1. For data obtained in the Mach reflection region, the air shock arrival times are plotted versus the ground range in Fig. 3.2. No data was obtained on Shot 3.

3.2 SECONDARY RESULTS

The secondary data obtained by Project 1.4 on this series of tests includes the peak pressures of the shock wave calculated from the average velocities across various sub-bases. To make these calculations, one must assume that the conditions of the Rankine-Hugoniot relations[3] existed along the sub-bases at the time of transit of the shock wave. Near the ground, in the region of regular reflection and particularly on Shot 4, the accuracy of this assumption is questioned.

The sub-bases between blast switches located at the same height above the ground and at successive stations along the blast line were used for the pressure calculations. The sub-bases between blast switches at different heights above the ground and at the same blast station were used for velocity and temperature computations. These velocities reveal differences in the layer of air near the ground in the vicinity of ground zero. Velocities obtained at one station in this manner were subject to such a great error due to the short distance used as a base line that peak pressures were not calculated in these intervals. The error was not so great, however, that the velocities could not be used for comparison purposes. These velocities in the free air region have been substituted in the Equation 1.4 to evaluate average air temperatures in the intervals as listed in Table 3.2.

3.2.1 Shot 1

The arrival times at Station F-202 indicate an increasing rather than decreasing velocity of the shock front as the front pro-

TABLE 3.1

Time of Shock Arrival

Shot	Station	50-foot level			10-foot level			Ground level		
		Arrival Time (sec)	Slant Range (feet)	Ground Range (feet)	Arrival Time (sec)	Slant Range (feet)	Ground Range (feet)	Arrival Time (sec)	Slant Range (feet)	Ground Range (feet)
1	F-200	None	756	139	0.3258	798	150	0.3325	807	150
1	F-202	0.4242	943	580	0.4484	976	583	0.4521	984	583
1	F-204	0.6961	1306	1073	0.7158	1331	1076	0.7161	1336	1076
1	F-206	1.0417	1738	1572	0.0546	1757	1572	1.0550	1762	1572
1	F-208	1.4251	2200	2070	1.4281	2215	2072	1.4281	2218	2072
1	F-210	2.2285	3158	3068	2.2302	3168	3070	2.2294	3171	3070
2	7-200	0.5187	1072	166	0.5473	1110	157	0.5534	1120	157
2	7-201	0.6445	1234	633	0.6701	1266	630	0.6761	1276	630
2	7-213	None	1460	1005	0.8424	1489	1003	0.8481	1496	1003
2	7-202	None	1738	1378	1.0622	1761	1377	1.0661	1768	1377
2	7-203	1.5748	2375	2126	1.5868	2393	2126	1.5861	2398	2126
2	7-204	None	3065	2876	2.1656	3079	2875	2.1659	3082	2875
4	7-200	None	1012	207	None	1053	213	None	1063	213
4	7-202	0.5182	1667	1342	0.5101	1693	1343	0.4941	1699	1343
4	7-204	1.4343	3006	2839	1.4343	3020	2839	1.4334	3024	2839
4	7-206	2.5421	4419	4338	2.5432	4459	4338	2.5424	4461	4338
4	7-208	3.7332	5920	5837	3.7350	5928	5837	3.7346	5929	5837
4	7-210	6.2340	8892	8837	6.2347	8897	8837	6.2347	8898	8837

UNCLASSIFIED

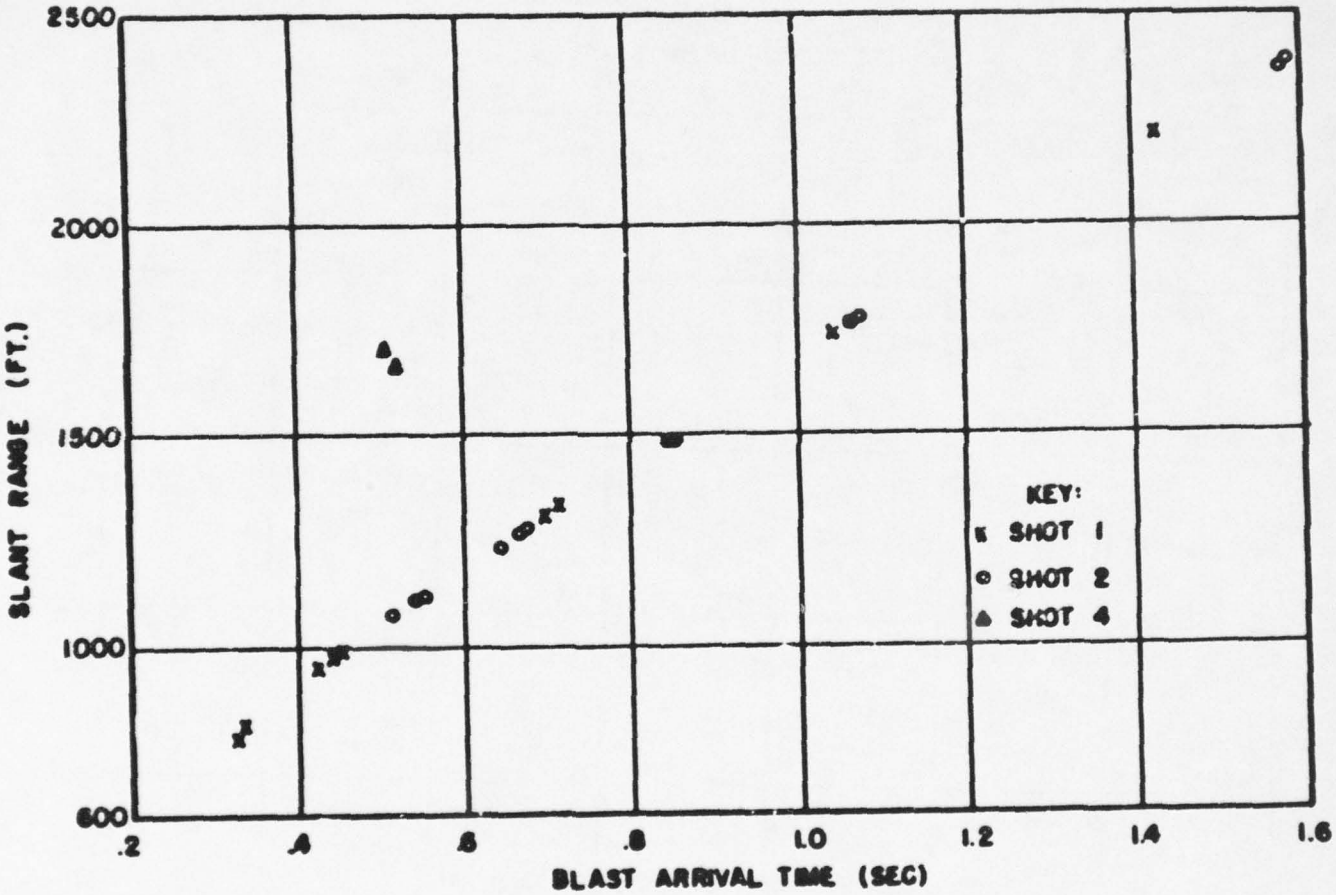


Fig. 3.1 Blast Arrival Times in Free Air

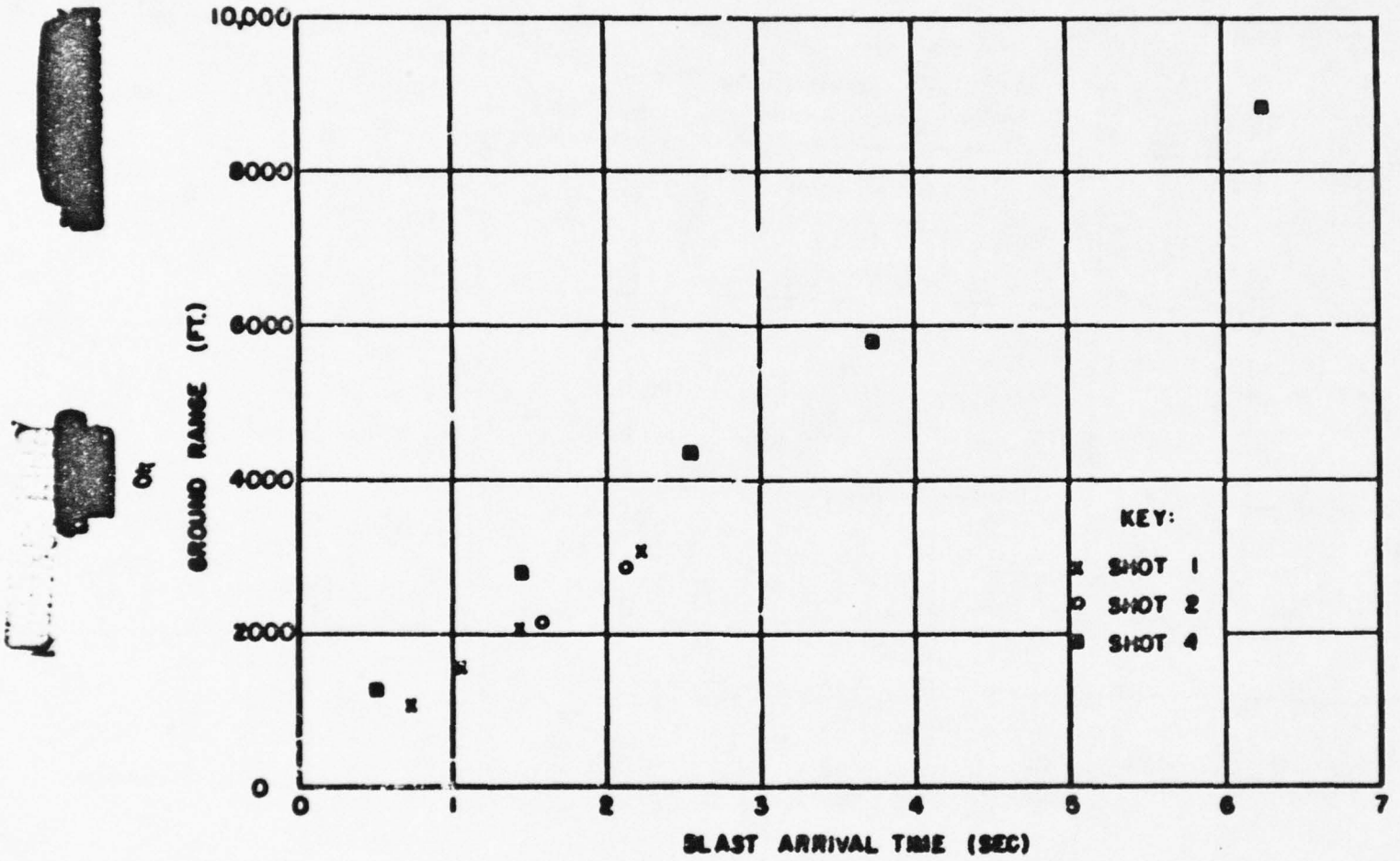


Fig. 3.2 Blast Arrival Times in Mach Region

UNCLASSIFIED

UNCLASSIFIED

TABLE 3.2

Air Temperature from Velocity Measurements

Shot	Station	Gage Height (feet)	Interval time (sec)	Interval Distance (feet)	Average Velocity (ft/sec)	Measured Pressure (psi)	Temperature (Degrees Centigrade)
1	F-200	10-0	0.0067	9	1313	7.10	12
1	F-202	50-10	0.0242	33	1364	6.66	16
1	F-202	10-0	0.0037	8	2164	6.23	495
2	7-200	50-10	0.0286	38	1329	5.38	26
2	7-200	10-0	0.0061	10	1639	5.16	186
2	7-201	50-10	0.0259	32	1236	4.40	-1
2	7-201	10-0	0.0057	10	1754	4.15	281
4	7-202	50-10	-0.0081				
4	7-202	10-0	-0.0160				

gresses from the 50 foot level to ground level. Specifically, the average velocity in the interval 50 feet to 10 feet was 1364 ft/sec; in the 10 ft to zero interval it was 2162 ft/sec. Using the pressures recorded at this station by pressure-time gages as a basis for interpolation, together with these average velocities, and Equation 1.4, the temperature in the upper and lower intervals were found to be 16° and 495° centigrade respectively. Even though use of Equation 1.4 is open to question, it is clear that a decided increase in temperature must have been present. In the Mach reflection region, the arrival times indicate a vertical Mach stem within the time resolution of the instrumentation.

3.2.2 Shot 2

The shock front arrival times in the free air region agree with those of Shot 1 (see Fig. 3.1). At Station 7-200, the calculated temperature indicated 26°C in the 50 ft to 10 ft interval and 186°C in the 10 ft to ground level interval. At 7-201, the temperature varied from roughly ambient in the upper interval to 281°C in the lower interval. The limitations of the instrumentation were such that this calculation should not be performed at stations farther out. Nearly all of

UNCLASSIFIED

TABLE 3.3

Shot 1

Stations	Blast Switch Height (ft)	Interval Distance (ft)	Interval Time (sec)	Average Shock Velocity (ft/sec)	Test Site Conditions			Corrected to 1 KT at Sea Level		
					Computed Pressure (psi)	*Slant Range (ft)	*Ground Range (ft)	Computed Pressure (psi)	Slant Range (ft)	Ground Range (ft)
200-202	50	No Measurement								
202-204	50	363	0.2719	1335	6.67	1110		7.60	1045	
204-206	50	432	0.3456	1250	3.94	1509		4.49	1421	
206-208	50	462	0.3834	1205	2.57	1957		2.93	1843	
208-210	50	998	0.8034	1242	3.69	Mach	2527	4.21	Mach	2380
200-202	10	178	0.1226	1452	10.72	882		12.22	831	
202-204	10	355	0.2674	1328	6.44	1139		7.34	1073	
204-206	10	**								
206-208	10	499	0.3735	1336	6.70	Mach	1806	7.64	Mach	1701
208-210	10	998	0.8021	1244	3.75	Mach	2527	4.28	Mach	2380
200-202	0	177	0.1196	1480	11.76	890		13.38	838	
202-204	0	**								
204-206	0	497	0.3369	1475	11.55	Mach	1304	13.17	Mach	1228
206-208	0	499	0.3731	1337	6.73	Mach	1806	7.67	Mach	1701
208-210	0	998	0.8013	1245	3.78	Mach	2527	4.31	Mach	2380

* Distances corrected by means of Equation 1.6

** Transition Zone

UNCLASSIFIED

TABLE 3.4

Shot 2

Station	Blast Switch Height (ft)	Interval Distance (ft)	Interval Time (sec)	Average Shock *Velocity (ft/sec)	Test Site Conditions			Corrected to 1 KT at Sea Level		
					Computed Pressure (psi)	*Slant Range (ft)	*Ground Range (ft)	Computed Pressure (psi)	Slant Range (ft)	Ground Range (ft)
200-201	50	162	0.1258	1285	4.97	1128		5.98	1012	
201-203	50	1142	0.9303	1222	3.07	1717		3.70	1540	
200-201	10	157	0.1231	1272	4.57	1186		5.50	1064	
201-213	10	222	0.1720	1285	4.97	1374		5.98	1232	
213-202	10	273	0.2198	1236	3.49	1620		4.20	1453	
202-203	10	631	0.5246	1196	2.32	2056		2.79	1884	
203-204	10	***								
200-201	0	156	0.1227	1268	4.45	1196		5.36	1073	
201-213	0	220	0.1720	1274	4.63	1382		5.57	1240	
213-202	0	272	0.2180	1242	3.67	1627		4.42	1459	
202-203	0	***								
203-204	0	749	0.5791	1285	4.97	Mach	2853	5.98	Mach	2559

Note: * Distances corrected by means of Equation 6
** Corrected for wind velocity component
*** Transition Zone

UNCLASSIFIED

UNCLASSIFIED

TABLE 3.5

Shot 4

Station	Blast Switch Height (ft)	Interval Distance (ft)	Interval Time (sec)	Average Shock Velocity (ft/sec)	Test Site Conditions			Corrected to 1 KT at Sea Level		
					Computed Pressure (psi)	*Slant Range (ft)	*Ground Range (ft)	Computed Pressure (psi)	Slant Range (ft)	Ground Range (ft)
200-202	50	No Measurement								
202-204	50	**								
204-206	50	1499	1.1078	1353	6.78	Mach	3522	8.13	Mach	1229
206-208	50	1499	1.1911	1259	3.88	Mach	5041	4.65	Mach	1759
208-210	50	3000	2.5008	1200	2.17	Mach	7206	2.60	Mach	2515
200-202	10	No Measurement								
202-204	10	**								
204-206	10	1499	1.1089	1352	6.75	Mach	3522	8.09	Mach	1229
206-208	10	1499	1.1918	1258	3.85	Mach	5041	4.62	Mach	1759
208-210	10	3000	2.4997	1200	2.17	Mach	7206	2.60	Mach	2515
200-202	0	No Measurement								
202-204	0	1496	0.9393	1593	15.13	Mach	1977	18.14	Mach	690
204-206	0	1499	1.1090	1352	6.75	Mach	3522	8.09	Mach	1229
206-208	0	1499	1.1922	1257	3.82	Mach	5041	4.58	Mach	1759
208-210	0	3000	2.5001	1200	2.17	Mach	7206	2.60	Mach	2515

Note: * Distances Corrected by means of Equation 6
** Transition Zone

UNCLASSIFIED

UNCLASSIFIED

TABLE 3.6

Test Conditions

	Shot 1	Shot 2	Shot 4
Location	FF Area	T-7 Area	T-7 Area
Date	1 April	15 April	1 May
Time	0900	0929	0929
RC Yield in KT	1.05	1.15	19.6
Direction of Blast Line from Station 200	W	S9°56'W	S9°56'W
Burst Position from Station 200	122 ft. N 67 ft. E	143 ft S 84 ft E	140 ft S 153 ft W
Burst Height	793	1109	1040
Scaled Height	747	995	363
Ambient Pressure at Ground Level (psi)	13.26	12.73	12.72
Ambient Pressure at Burst Height (psi)	12.89	12.21	12.26
Ambient Temperature at Ground Zero (°C)	1.44	12.3	17.0
Computed Sound Velocity (ft/sec)	1116	1112.3	1121.4
Wind Velocity (mph)	4.6	6.5	2.5
Wind Direction	N	NNW	SSW

UNCLASSIFIED

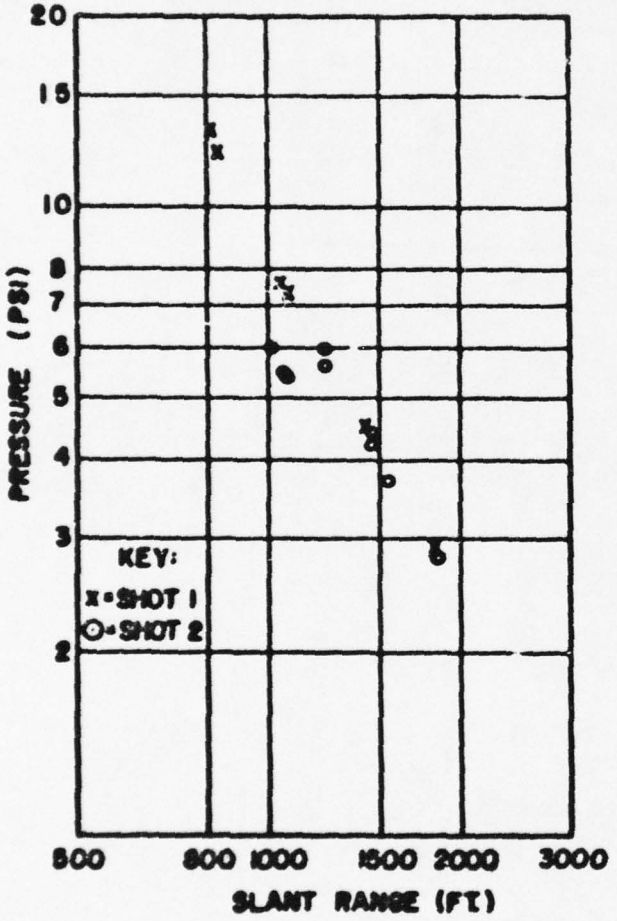


Fig. 3.3 - Free Air Pressure vs. Distance, Corrected to 1 KT at Sea Level.

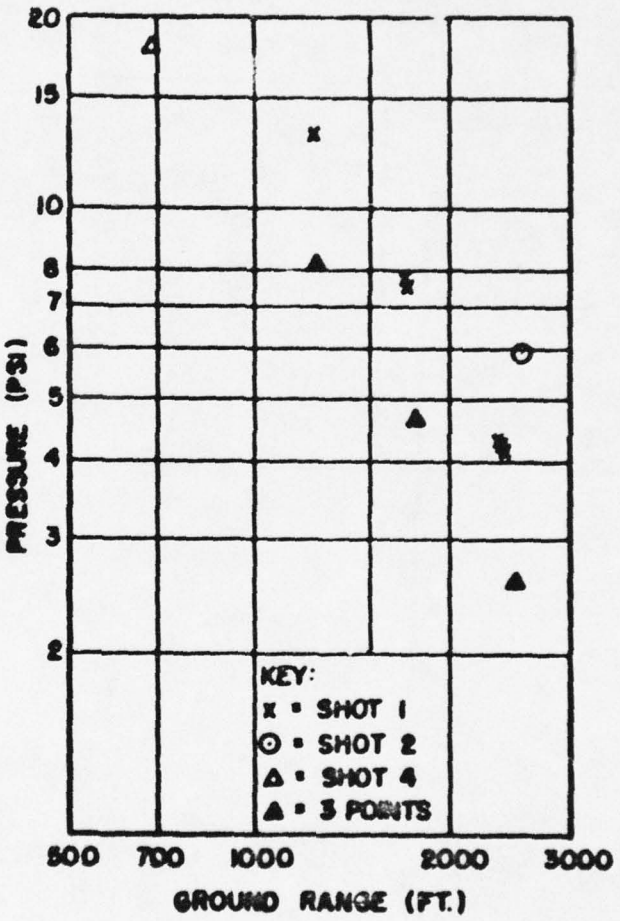


Fig. 3.4 - Mach Pressure vs. Distance, Corrected to 1 KT at Sea Level.

UNCLASSIFIED

the stations were placed in the region of regular reflection for this shot so that no data was available on Mach stem characteristics.

3.2.3 Shot 4

Blast switches for Shot 4 were placed primarily in the Mach region. The three switches at Station 7-200 failed to operate, resulting in a major loss of information in the region of regular reflection. This failure was probably due to the effects of the bomb at close range. The blast switch at the 10-foot level of Station 7-202, was activated 16 milliseconds after the ground level switch closed and 8 milliseconds before the 50-foot blast switch closed. This information substantiates the existence of a precursor to the main shock which was indicated on the various pressure-time systems in the free air region and was observed in some of the photographs made by EG&G.

The propagation of the Mach stem is indicated by the blast arrival times. At Station 7-204, the triple point was above 50 ft. and the Mach stem was moving down the blast line as a vertical front. The arrival times at the remaining stations indicate that the Mach stem was vertical at least as far as Station 7-210.

3.2.4 Peak Pressures

The results of the computation of peak pressures from arrival time data are listed in Tables 3.3, 3.4 and 3.5, with sufficient information in Table 3.6 so that the reader can perform the calculations. The free air pressures versus slant ranges corrected to 1 KT at sea level may be seen in Fig. 3.3. Figure 3.4 presents Mach pressure as a function of ground range reduced to 1 KT at sea level. The pressures for the height of burst curves in Fig. 3.5 were taken from Fig. 3.4. In correcting to sea level, all computations were based on atmospheric conditions supposedly existing at burst height to permit comparison of data with other projects. Blast efficiencies were calculated from the free air measurements of Shots 1 and 2 by the relation given in Equation 2.5 and are listed in Table 3.7.

The computation of pressures from the air shock arrival times was based on the assumption that the Rankine-Hugoniot relationships were applicable and that the medium through which the shock wave was propagated was homogeneous. The latter assumption is questionable, especially along a base line several thousand feet in length. When an atomic bomb explodes, the radiation from the fireball heats all surfaces exposed to it. In the region around ground zero, this heating is sufficient to cause significant quantities of dust, smoke, and water

UNCLASSIFIED

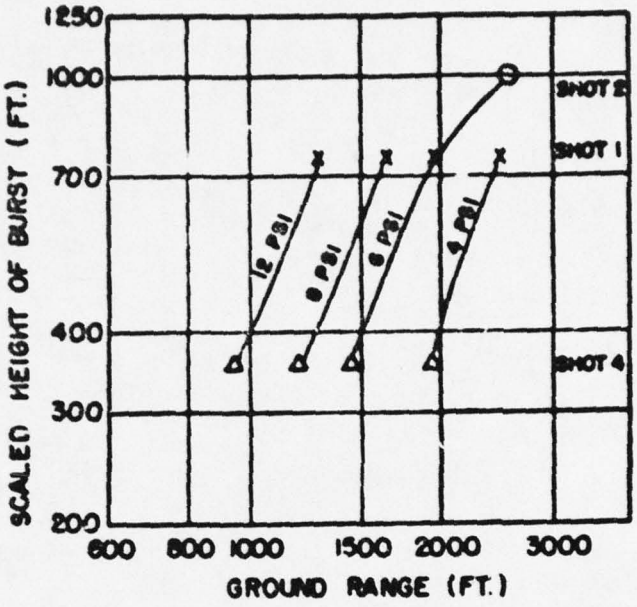


Fig. 3.5 Height of Burst Curves Corrected to 1 KT at Sea Level

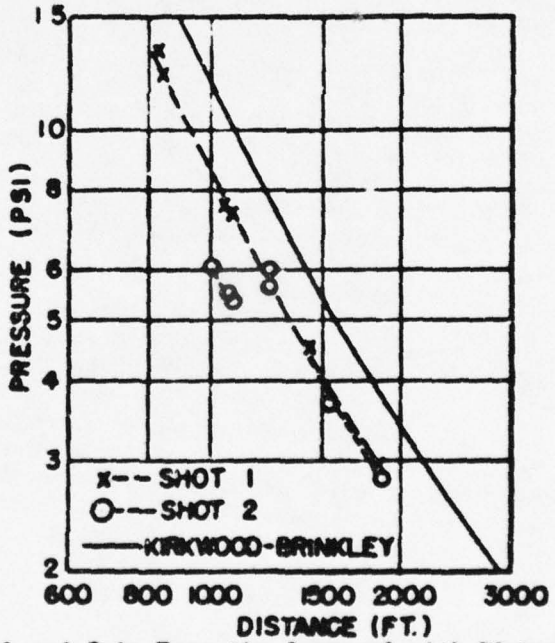


Fig. 3.6 Shots 1 and 2 in Free Air Compared with Kirkwood-Brinkley Spherical Unit TNT Curve Scaled to 1 KT

UNCLASSIFIED

TABLE 3.7

Blast Efficiencies

Shot	Slant Range (ft)		Free Air Pressure (psi)	Blast Efficiency $E = \left[\frac{R_v}{R_{K.B.}}\right]^3$
	R_v	$R_{K.B.}$		
1	~~8983~~ 8	926	13.38	~~89~~ 74
1	~~8823~~ 1	970	12.22	~~75~~ 63
1	~~1110~~ 45	1222	7.60	~~75~~ 62.5
1	~~1239~~ 93	1247	7.34	~~76~~ 64
1	~~1509~~ 21	1676	4.49	~~75~~ 61
1	~~1957~~ 14	2218	2.93	~~69~~ 57
2	1012	1399	5.98	38
2	1232	1399	5.98	68
2	1240	1474	5.57	59
2	1064	1481	5.50	37
2	1073	1487	5.36	38
2	1459	1676	4.42	66
2	1453	1764	4.20	56
2	1560	1903	3.70	53
2	1844	2300	2.79	52

R_v - Measured

$R_{K.B.}$ - Kirkwood-Brinkley Theoretical

vapor to be added to the air. A temperature increase in the medium causes a decrease in density and an increase in ambient pressure which may or may not reach equilibrium again before the arrival of the shock wave.

On the other hand, the addition of water vapor, dust, and smoke to the air would increase the absolute density of the air. Whether this m dium would still obey the ideal gas law is an additional question. In view of these factors, the computation of pressures from

UNCLASSIFIED

velocity measurements in the region very close to the ground does not appear feasible.

The configuration of the blast line with respect to the point of detonation of the bomb, as shown in Fig. 3.7 is such that the effective sub-bases used for velocity determinations in the free air region are high above the ground where the temperature and dust effects should be small. This was true even for pressures computed from arrival times measured at ground level. Near ground zero, where the effective sub-bases were comparatively short, there is a possibility of some error in the computed pressure due to the change in velocity of the shock front in the heated layer of air near the ground.

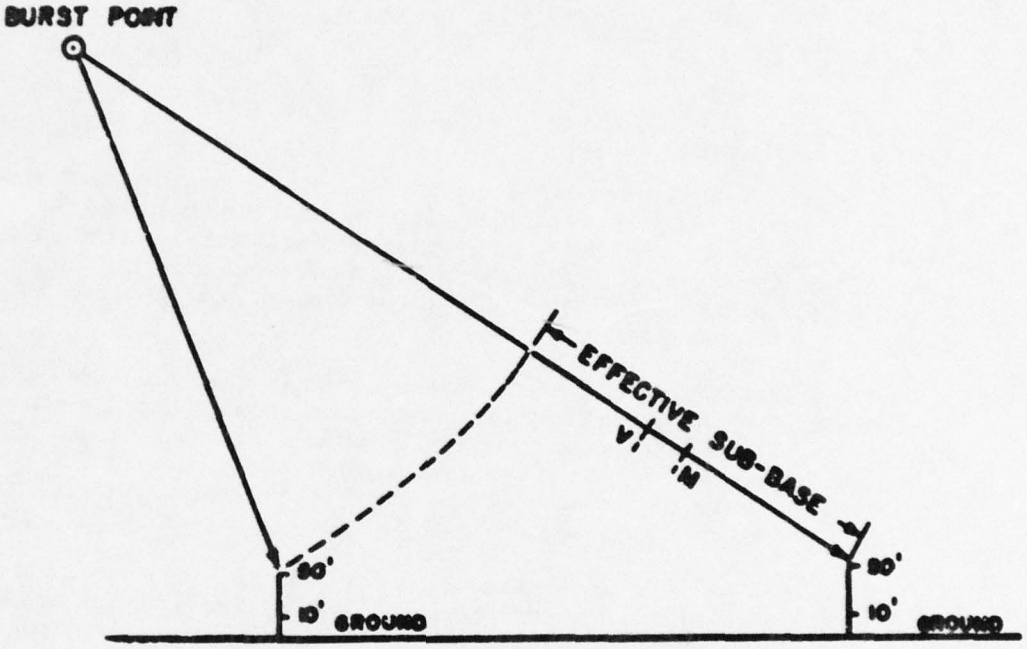
The free-air pressure-distance curves obtained on Shots 1 and 2 were fitted by eye. These curves were compared to the Kirkwood-Brinkley curve for TNT in Fig. 3.6. The pressures obtained on Shot 2 for the sub-bases nearest the bomb, are low. These values were obtained at the point where the maximum error in the velocity system would be expected.

In the region of Mach reflection of the shock wave, the effective sub-base lengths were essentially the same as the distances along the ground between successive blast stations. The location of the Mach reflection region with respect to ground zero is such that the radiation from the bomb probably had small effect. The pressures computed in the Mach reflection region on Shots 1, 2 and 4 were in good agreement with expected pressures.

3.2.5 Blast Efficiencies

The blast efficiencies for Shots 1 and 2 were computed on the basis of Radiochemical yields of 1.05 KT and 1.15 KT for Shots 1 and 2 respectively. A blast efficiency was computed for each free air pressure determination on both shots. No blast efficiencies were computed for Shot 4 since no free-air pressures were obtained for that test. The best single value of blast efficiency for a given bomb would be that value obtained for a free-air pressure of 10 psi. On the basis of the value shown in Table 3.7 and Fig. 3.6, this efficiency for Shot 1 is 75 per cent. The pressure nearest 10 psi for Shot 2 indicates a blast efficiency of 68 per cent with considerable variation for the lower pressures.

UNCLASSIFIED



M - MID-POINT OF SUB-BASE
V - POINT AT WHICH AVERAGE VELOCITY EQUALS INSTANTANEOUS VELOCITY

Fig. 3.7 Configuration of Effective Sub-base Length in Free Air

UNCLASSIFIED

SECRET

CHAPTER 4

CONCLUSIONS AND RECOMMENDATIONS

4.1 CONCLUSIONS

The air shock arrival times clearly indicate that the shock front velocity near the ground was faster than it was between 10 and 50 feet above the ground in the region of regular reflection near ground zero. This effect was noted on Shots 1 and 2. No data was obtained on Shot 3. The data obtained in this region on Shot 4 was not applicable due to the presence of a precursor wave.

The increased velocities noted were probably due to a layer of heated air near the ground caused by radiation from the bomb. Since the pressure-time data taken by other agencies indicate no great differences in pressure in these two levels, the increased velocities can be attributed only to increased temperature of the medium through which the shock wave was propagated.

If we assume that the Rankine-Hugoniot relations are applicable in this region, and use the pressures obtained by the agencies who were measuring the pressure-time relations of the shock waves, then the average temperatures corresponding to these increased velocities may be approximated. Temperatures of several hundreds of degrees centigrade in the layer of heated air within 10 feet of the ground were found.

The air shock arrival times on Shot 4 corroborate the existence of the precursor shock wave observed on the pressure-time records and the EG&G photographs. The arrival of a shock wave at the ground level blast switch, the 10-foot level, and the 50-foot level, in that order, was noted at Station 7-202 on Shot 4.

The air shock arrival times indicated that the Mach stem was vertical as it moved down the blast line for Shots 1 and 4. Not enough data was obtained in the Mach reflection region of Shot 2 to determine the slope of the Mach stem.

The blast efficiency determinations on Shots 1 and 2 indicated efficiencies of the order of 75 and 68 per cent respectively. No blast efficiency was computed for Shot 4 because no free-air pressures

SECRET

UNCLASSIFIED

were obtained.

The Mach pressures obtained on Shots 1 and 4 are in fair agreement with predicted curves.

4.2 RECOMMENDATIONS

The air shock arrival times recorded by the pressure-time measuring systems for this series of shots should be used to determine the approximate temperatures along the blast line at the time of transit of the shock wave. This can be done by means of the Rankine-Hugoniot relationship as stated in Equation 1.4.

Any future tests that require air shock arrival time measurements should be instrumented to obtain as many arrival times as practicable. If these arrival times are to be used to calculate pressures, careful determination of the conditions of the air at the time of transit of the shock wave must also be made.

UNCLASSIFIED

PART II

FEASIBILITY TEST OF RADIO TELEMETRIC SYSTEM FOR MEASURING AIR BLAST ARRIVAL TIMES ON AN ATOMIC DETONATION

BY

NICHOLAS M. MASICH, LT COL, USAF
WALTER F. MOLESKY, LT COL, SIGC
WILLIAM L. BOWNE, LT, USN

ACKNOWLEDGMENTS

The work entailed in adaptation of the radiotelemetric equipment, its installation for the test, the reduction of data and the writing of Part II of this report was performed by:

Nicholas M. Masich, Lt Col, USAF
Walter F. Molesky, Lt Col, SigC
William L. Bowne, LT, USN
John R. Mackey, Pfc. USA
William T. Matthews

The encouragement of Dr. R. R. Minor, Chief of the Explosion Kinetics Branch, Ballistic Research Laboratories spurred the efforts of the above group.

UNCLASSIFIED

CHAPTER 5

INTRODUCTION

5.1 OBJECTIVE

The main purpose of the work discussed in Part II was to investigate the feasibility of using a directional radio telemetric system for determining blast arrival time data from nuclear detonations.

5.2 GENERAL

The use of blast arrival times to determine peak air pressures has been made on many previous atomic explosions. The theory is given in the air pressure reports for Operation GREENHOUSE[9] and Operation JANGLE[10]. The Explosion Kinetics Branch of the Ballistic Research Laboratories participated on Shot 6 of Operation TUMBLER-SNAPPER in order to conduct a feasibility test of a directional radio telemetric system adapted by this group. Previous work with a modified standard telemetering system was reported in connection with Operation GREENHOUSE by Colonel Frolich[11] which proved that telemetering in general was feasible. This system was omnidirectional, however, and did not take full advantage of the inherent possibilities of pulse transmission techniques.

The use of cable installations for measuring blast arrival times is inordinately expensive. Projects which include water areas in the blast lines further preclude the use of cable. Prior to entering an extensive development program, it was decided that suitable tests on existing ultra-high-frequency equipment, properly modified, should be performed to determine the effects of radiation upon such a system.

5.3 BASIC PLAN

The fundamental instrumentation plan consists of a foil switch, transmitter, receiver and recorder. Upon closure of the foil switch, the transmitter sends out a short duration pulse which is picked up by the receiver from whose output the signal is processed on a magnetic tape.

CHAPTER 6

INSTRUMENTATION

6.1 OVERALL SYSTEM

The test system was composed of two specially built components and several modified or adapted parts. The blast switches were designed for the particular task, as was a signal processing circuit between the output of the receiver and the recorder. The transmitters were modified U. S. Navy BuOrd Shore Bombardment Beacons, Mark II Mod 1, and the receiver was an AN/APR-4 pulse receiver. The processed output of the receiver was applied to the tape recorder through an amplifier and mixing bridge to introduce a 10 kc timing wave.

6.1.1 Blast Switch

An aluminum foil switch adapted for insertion into a 1 1/2 inch conduleT was developed to permit ease of installation onto a pipe standard, and to shade the foil from direct thermal radiation. Figure 6.1 shows this switch fully assembled for mounting on a pipe. Figure 6.2 shows the basic components, conduleT with insulator and center conductor, foil mount, and protective shield which screws on over insulator. The aluminum foil was 1 millimeter thick, perforated, and had been tested to close and rupture under a pressure of 2 psi within a non-critical time of a few microseconds. The switch was normally open, closed upon arrival of the blast wave, and ruptured to open permanently from the effect of the blast. Calibration was based on a series of experiments which indicated the extent of perforation required to effect such rupture. Because any test would destroy the particular piece of foil, exact calibration was impossible and specifications to meet minimum requirements could be the only result.

6.1.2 Transmitter

The U. S. Navy Radar Beacon, with the receiver function disabled, was used as the transmitter. A schematic diagram of this equipment is shown in Fig. 6.3. The beacon operated in the frequency band from 900 to 1000 mc with a peak pulse output power of 15 watts to the antenna feed line. The antenna system consisted of a half-wave dipole with corner reflector mounted on a 30 ft. mast to provide a 60° by 90°

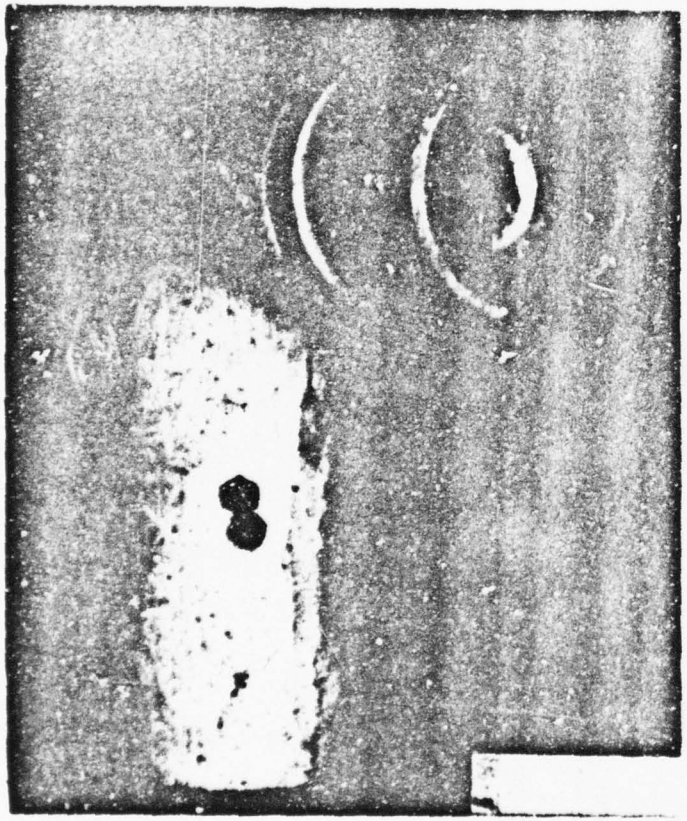


Fig. 6.1 Aluminum Foil Switch

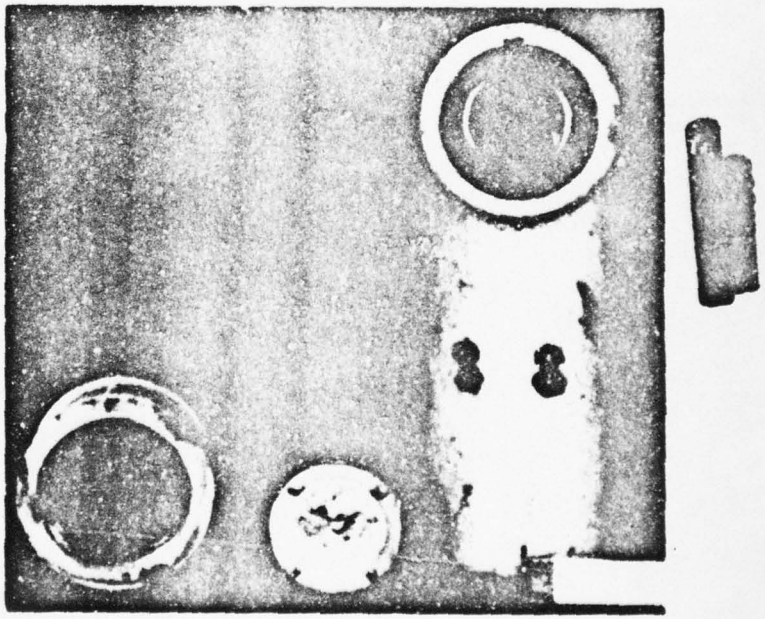


Fig. 6.2 Basic Components of Foil Switch

beam width. The antenna was coupled to the transmitter by 40 ft. of type RG-8/U UHF cable.

The power supply for the transmitter consisted of a 6-volt storage battery. The filaments were supplied directly from the battery; the high voltages required were obtained from a dynamotor located in the control box.

The control box was modified to allow sequential turning on of the power requirements automatically at each transmitting station. This was achieved with a 12 hour mechanical clock used to turn on the filament power at a pre-set time and an Amperite thermal delay relay actuated by the same closure which turned on the plate power after a 60 second delay.

The receiver section of the Radar Beacon was disabled by pulling the quench oscillator 6C4(V1) and the video amplifier 6C4(V4) tubes.

The 6F4(V2) oscillator tube was mounted in a half-wave coaxial line as circuit elements operating as a Colpitts oscillator. The oscillator was normally non-operative until a voltage pulse, formed by discharging a pulse forming line, was applied to the plate through the modulation transformer. The discharge circuit included a 2D21(V6) thyratron which was controlled by the blocking oscillator tube 6C4(V5). The blocking oscillator tube was triggered by the blast switch which when momentarily closed, short circuited resistor R9 reducing the grid bias to zero thus providing a positive pulse to the grid of the thyratron. This thyratron was so connected as to be self-recovering after discharge of the pulse forming line.

A separate, portable, 1000 cycle test oscillator was used in place of the blast switch for testing and ranging the system.

6.1.3 Receiver

The receiver used was the AN/APR-4 with tuning unit TN18 covering 300 to 1000 mc. The transmitters were both tuned to the same frequency, 955 mc, using the receiver set on narrow bandwidth to check operation. The receiver was then turned on to broad band operation so that uneven drift in the tuning of the various units would not prevent reception. Because of the short duration of the transmitted pulse and the presence of appreciable background noise, direct recording of the receiver output was impossible. To overcome this difficulty a "black box" pulse processing circuit was built which amplified the received

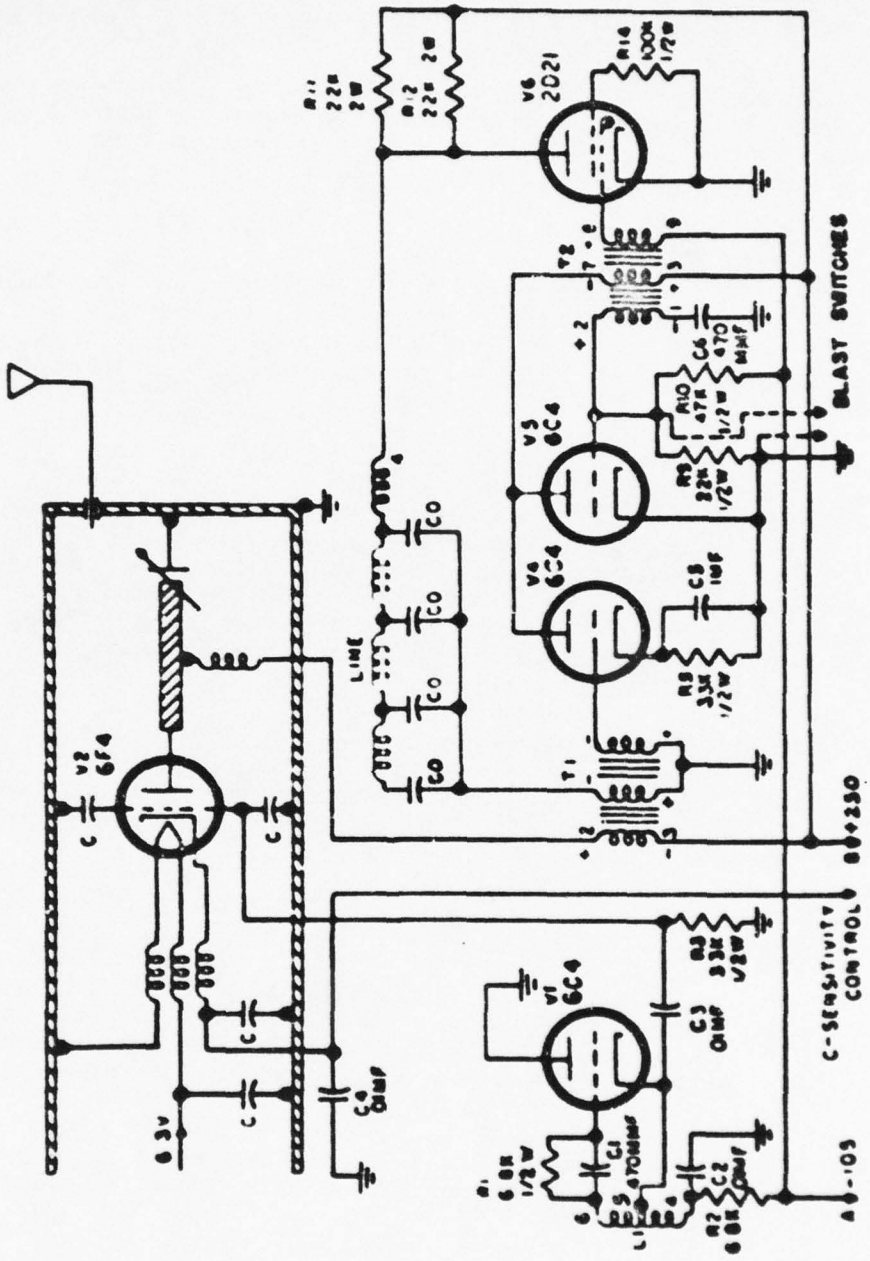


FIG. 6.3 BEACON TRANSMITTER

signal pulse and reduced noise in a stage normally biased beyond cut-off; the remaining signal pulse then triggered a one-shot multivibrator which broadened the pulse sufficiently for recording. This circuit is shown schematically in Fig. 6.4.

6.1.4 Recording

The output of the "black box", taken off the plate of the normally conducting tube of the multivibrator was fed through an amplifier chassis and mixing bridge to the recording head. Recorders used were of the Magnacorder type. A crystal controlled 10 kilocycle timing wave was also introduced through a mixing bridge to the same recording head.

6.1.5 Monitoring

During preliminary check-outs as well as the actual test, an oscilloscope was connected across the recording head. During the test, the sweep voltage was derived from the line frequency of the gasoline powered motor generator used to obtain 60-cycle power, thus maintaining constant screen illumination at the expense of having a sine wave (non-linear) sweep.

6.1.6 Permanent Record

A permanent record was made on 35 mm film by playing back the recording through an oscilloscope. The oscilloscope pattern was photographed with a high speed camera.

6.1.7 Blast Line Layout

The blast line set up for this test was as follows. Blast switches were placed at 1200, 1500, and 2000 ft. from ground zero to actuate a transmitter at 2100 ft; and at 2500, 3000, and 3500 ft. to actuate a transmitter at 3600 ft. These switches were placed approximately 1 ft. above ground. These positions were not closely surveyed, but were on a radial line south of ground zero. The transmitters were placed beyond the association switches to permit functioning prior to the arrival of the air blast, thus avoiding the possibility of non-transmittal of the arrival pulses through damage to transmission equipment or antennae.

The receiving station was approximately 10 miles from the transmitters. Its position was not more than 15° east of the radial blast line and its elevation provided a good line of sight.

UNCLASSIFIED

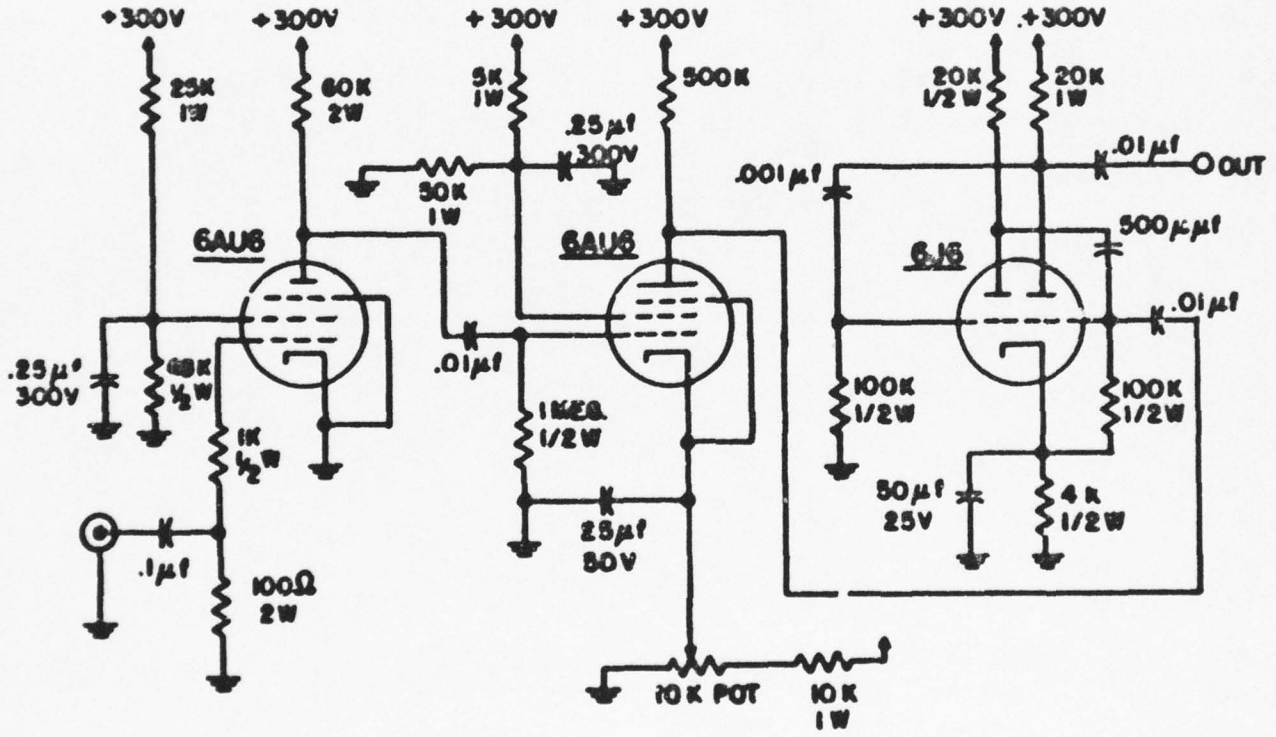


Fig. 6.4 Pulse Processing Circuit

UNCLASSIFIED

UNCLASSIFIED

CHAPTER 7

TEST RESULTS

7.1 EQUIPMENT PERFORMANCE AND OBSERVATIONS

Results of this test indicated that a directional radio telemetric system in the ultra-high frequency region is feasible for blast arrival time measurements for a nuclear explosion.

Detailed analysis of equipment performance actually consisted of bringing together the inconclusive results of visual monitoring at the receiving station during the test and surveying conditions on the blast line after the shot. The permanent record was unsatisfactory for detailed study because of the amount of noise interference.

7.1.1 Visual Monitoring

The most important visual monitoring result was the immediate determination that there was no blocking of reception due to intense radiation even though the receiving antenna was directed toward the nuclear burst. Of equal value to subsequent study was the determination of the nature of observed interference which obscured later analysis of the permanent record. Strong noise signals persisted continuously from the time the receiving station was turned on, approximately 1 1/2 hours before the shot, until operations were suspended about 10 minutes after the shot. Most of this interference was seen to synchronize with the sine-wave sweep derived from the motor generator set.

Since this noise interference had not occurred on prior checks, it was a last minute handicap which could not be cured in the limited time remaining before the shot. A quick check indicated that the receiver pulled in this noise, and that if higher powered transmitters had been available, a lower gain setting on the receiver would have eliminated most or all such spurious pulses. However, in this test, such an expedient would also have eliminated reception of data.

The last important observation was the fact that pulses were transmitted and received in this system under shot conditions. Again, the sine-wave sweep helped indicate the different timing of

UNCLASSIFIED

UNCLASSIFIED

these pulses from the long observed noise, but hindered determination of the number of such data pulses due to crowding at one end of the non-linear sweep.

7.1.2 Recovery Party Observations

The recovery party entered the blast area at the earliest possible time after the shot to recover equipment and observe conditions. In short, it was found that the foils of the switches at 1200 and 1500 ft. had been melted by heat, although shaded from direct radiation, with no probability of either having closed to produce data transmission. The switch at 2000 ft. was severely punctured, though not ruptured, indicating definite transmission. The switch at 2500 ft. was not punctured or ruptured, but a faint nipple indicated a probable closure. The switch foils at 3000 and 3500 ft. remained taut with no indication of any contact having been made. This led to the conclusion that only two data pulses had been observed on the monitoring scope. Although the foil switch design had been tested to rupture the foils at 2 psi in a shock tube, unknown field conditions and weaknesses in the switch design prevented this at even higher anticipated overpressures.

In addition to switch conditions, it was noted that the antenna at 2100 ft. was blown away, and the mast broken into three sections lying on the ground away from ground zero. No damage to either transmitter and associated parts which were buried at the foot of each mast was observed.

7.1.3 Playback Results

Playback of the magnetic tape showed a disturbing amount of noise signals. The data pulses were not clearly identifiable in the photographic record.

UNCLASSIFIED

UNCLASSIFIED

CHAPTER 5

CONCLUSIONS AND RECOMMENDATIONS

5.1 CONCLUSIONS

This test proved the feasibility of directional UHF radio telemetering for determining blast arrival time data from nuclear detonations. This was supported by the observation that transmitted blast switch pulses were received without being swamped by radiation from the burst. However, the modified beacon system as used in this test was found inadequate in the reported shot because of inherent power limitations and switch failure. Disruptive noise signals which obscured identification of the blast arrival time data on the permanent record was clearly determined to originate in local power sources and was definitely not associated with the detonation of the nuclear weapon.

5.2 RECOMMENDATIONS

Equally as important as the positive results of this test are the lessons learned from the negative results. From these, definite recommendations toward the design of suitable equipment for regular use in future tests can be made.

The basic principles of the foil switch are still important. That is, the switch is to be normally open, close momentarily on blast wave arrival, then open permanently. However, foil must be replaced by a substance which will not melt or break prematurely close to a bomb burst, yet which will function reliably under low blast pressures. To this end further development is a prerequisite.

The transmitters to be designed can follow the basic outline of the modified beacon units, but must incorporate a higher peak power output and broader pulse length. The pulse should be at least 50 watts peak power with a width of approximately 25 microseconds. Certain additional features, such as different pulse lengths for transmitter identification, an internal test modulator, and a self-initiation timer can be incorporated. In addition, great care must be exercised to insure that the frequency can be adjusted accurately and will maintain high stability.

The antenna system used in this test proved to be quite satisfactory. Similar units can be built for the proposed transmitters, remembering that they must be designed to function efficiently with the specific equipment.

It is anticipated that a more compact, narrower band receiver can be built to operate with specific transmission equipment with a considerable reduction in noise interference and additional processing circuits.

It is further recommended that power for the receiving station be supplied from a remotely located generator source in order to further reduce radiated noise interference from the generator itself.

UNCLASSIFIED

BIBLIOGRAPHY

1. Bryant, E. J., and Eberhard, R. A., and Kingery, C. N., Mach Reflection Over Hard Ground and Dry Sand, BRL Report 809

2. Carr, T. D., and Scharschild, M., and Weiss, P., An Improved Method for the Measurement of Blast from Bombs, BRL 336

3. Courant, R., and Friedrich, K. O., Supersonic Flow and Shock Waves, Interscience Publishers, Inc., New York

4. Eberhard, R. A., Kingery, C. N., and Molesky, W. F., Peak Air Blast Pressures from Shock Velocity Measurements along the Ground, Operation Buster-Jangle, Project 1.7a

5. Frankel, G. K., Apparatus for the Measurement of Air Blast Pressure by Means of Piezoelectric Gauges, NDRC A-373, OSRD 6251

6. Kirkwood, J. G., and Brinkley, S. R., Jr., Theoretical Blast Wave Curves for Cast TNT, NDRC A-341, OSRD 5481

7. Capabilities of Atomic Weapons, Supplement No. 1, TM 23-200, [illegible]-P-36-00100, AFCAT 385.2

8. Scientific Directors Report, Operation Greenhouse

9. W. H. Curtis, "Determination of Mach-Region Peak Blast Pressures from Shock-Velocity Measurements" Annex 1.6, Part III, Sec. 1 GREENHOUSE.

10. W. F. Molesky, R. A. Eberhard, C. N. Kingery, "Peak Air Blast Pressures from Shock Velocity Measurements along the Ground" RD Report Operation JANGLE, Project 1, 2a-1, WT-323.

11. A. Frolich, "Measurement of Free Air Peak Pressures by Telemetering from Mo,red Balloons", Annex 1.6, Part II, Sec. 2 of Air Blast Measurements, Operation GREENHOUSE.

[illegible]

UNCLASSIFIED

UNCLASSIFIED

DISTRIBUTION

	Copy No.
ARMY ACTIVITIES	
Asst. Chief of Staff, G-2, D/A, Washington 25, D. C.	1
Asst. Chief of Staff, G-3, D/A, Washington 25, D. C. ATTN: Dep. Asst. CofS, G-3, (RR&SW)	2
Asst. Chief of Staff, G-4, D/A, Washington 25, D. C.	3
Chief of Ordnance, D/A, Washington 25, D. C. ATTN: ORDTX-AR	4
Chief Signal Officer, D/A, P&O Division, Washington 25, D. C. ATTN: SIGOP	5- 7
The Surgeon General, D/A, Washington 25, D. C. ATTN: Chairman, Medical R&D Board	8
Chief Chemical Officer, D/A, Washington 25, D. C.	9- 10
Chief of Engineers, D/A, Military Construction Division, Protective Construction Branch, Washington 25, D. C. ATTN: ENGEB	11
Chief of Engineers, D/A, Civil Works Division, Washington 25, D. C. ATTN: Engineering Division, Structural Branch	12
The Quartermaster General, CBR, Liaison Office, Research and Development Division, D/A, Washington 25, D. C.	13
Office, Chief of Transportation, D/A, Washington 25, D. C. ATTN: Military Planning and Intelligence	14
Chief, Army Field Forces, Ft. Monroe, Va.	15- 17
Army Field Forces Board #1, Ft. Bragg, N. C.	18
Army Field Forces Board #2, Ft. Knox, Ky.	19
Army Field Forces Board #4, Ft. Bliss, Tex.	20
Commanding General, First Army, Governor's Island, New York 4, N. Y. ATTN: G-4, ACofS	21- 23
Commanding General, Second Army, Ft. George G. Meade, Md. ATTN: AIABB	24
Commanding General, Second Army, Ft. George G. Meade, Md. ATTN: AIAMX	25
Commanding General, Second Army, Ft. George G. Meade, Md. ATTN: AIACM	26
Commanding General, Third Army, Ft. McPherson, Ga. ATTN: ACofS, G-3	27- 28
Commanding General, Fourth Army, Ft. Sam Houston, Tex. ATTN: G-3 Section	29- 30
Commanding General, Fifth Army, 1660 Hyde Park Blvd., Chicago 15, Ill. ATTN: ALFEN	31
Commanding General, Fifth Army, 1660 Hyde Park Blvd., Chicago 15, Ill. ATTN: ALFOR	32
Commanding General, Fifth Army, 1660 Hyde Park Blvd., Chicago 15, Ill. ATTN: ALFMD-O	33- 36

[redacted] [redacted]

UNCLASSIFIED

UNCLASSIFIED

DISTRIBUTION (Continued)

	Copy No.
Commanding General, Sixth Army, Presidio of San Francisco, Calif. ATTN: AMGCT-4	37
Commander-in-Chief, European Command, APO 403, c/o PM, New York, N. Y.	38
Commander-in-Chief, U. S. Army Europe, APO 403, c/o PM, New York, N. Y. ATTN: OPOT Division, Com. Dev. Branch	39- 40
Commander-in-Chief, Far East Command, APO 500, c/o PM, San Francisco, Calif. ATTN: ACofS, G-3	41- 45
Commanding General, U. S. Army Alaska, APO 942, c/o PM, Seattle, Wash.	46
Commanding General, U. S. Army Caribbean, APO 834, c/o PM, New Orleans, La. ATTN: CG, USARCARIB	47
Commanding General, U. S. Army Caribbean, APO 834, c/o PM, New Orleans, La. ATTN: CG, USARFANT	48
Commanding General, U. S. Army Caribbean, APO 834, c/o PM, New Orleans, La. ATTN: Cml. Off., USARCARIB	49
Commanding General, U. S. Army Caribbean, APO 834, c/o PM, New Orleans, La. ATTN: Surgeon, USARCARIB	50
Commanding General, USAR Pacific, APO 958, c/o PM, San Francisco, Calif. ATTN: Cml. Off.	51- 52
Commanding General, Trieste U. S. Troops, APO 204, c/o PM, New York, N. Y. ATTN: ACofS, G-3	53
Commandant, Command and General Staff College, Ft. Leavenworth, Kan. ATTN: ALLIS(AS)	54- 55
Commandant, The Infantry School, Ft. Benning, Ga. ATTN: C.D.S.	56- 57
Commandant, The Artillery School, Ft. Sill, Okla.	58
Commandant, The AA&GM Branch, The Artillery School, Ft. Bliss, Tex.	59
Commandant, The Armored School, Ft. Knox, Ky. ATTN: Classified Document Section, Evaluation and Res. Division	60- 61
Commanding General, Medical Field Service School, Brooke Army Medical Center, Ft. Sam Houston, Tex.	62
Commandant, Army Medical Service School, Walter Reed Army Medical Center, Washington 25, D. C. ATTN: Dept. of Biophysics	63
The Superintendent, United States Military Academy, West Point, N. Y. ATTN: Professor of Ordnance	64- 65
Commanding General, The Transportation Corps Center and Ft. Eustis, Ft. Eustis, Va. ATTN: Asst. Commandant, Military Sciences and Tactics	66
Commandant, Chemical Corps School, Chemical Corps Training Command, Ft. McClellan, Ala.	67
Commanding General, Research and Engineering Command, Army Chemical Center, Md. ATTN: Special Projects Officer	68
RD Control Officer, Aberdeen Proving Ground, Md. ATTN: Director, Ballistics Research Laboratory	69- 70

UNCLASSIFIED

UNCLASSIFIED

DISTRIBUTION (Continued) — Copy No.

Commanding General, The Engineer Center, Ft. Belvoir, Va.
ATTN: Asst. Commandant, The Engineer School — 71- 73
Chief of Research and Development, D/A, Washington 25, D. C. — 74
Commanding Officer, Engineer Research and Development Laboratory, Ft. Belvoir, Va. ATTN: Chief, Technical Intelligence Branch — 75
Commanding Officer, Picatinny Arsenal, Dover, N. J.
ATTN: ORDBB-TK — 76
Commanding Officer, Army Medical Research Laboratory, Ft. Knox, Ky. — 77
Commanding Officer, Chemical Corps Chemical and Radiological Laboratory, Army Chemical Center, Md.
ATTN: Technical Library — 78- 79
Commanding Officer, Transportation R&D Station, Ft. Eustis, Va. — 80
Commanding Officer, Psychological Warfare Center, Ft. Bragg, N. C. ATTN: Library — 81
Asst. Chief, Military Plans Division, Rm 516, Bldg. 7, Army Map Services, 6500 Brooks Lane, Washington 25, D. C. ATTN: Operations Plans Branch — 82
Director, Technical Documents Center, Evans Signal Laboratory, Belmar, N. J. — 83
Director, Waterways Experiment Station, PO Box 631, Vicksburg, Miss. ATTN: Library — 84
Director, Operations Research Office, Johns Hopkins University, 6410 Connecticut Ave., Chevy Chase, Md.
ATTN: Library — 85

NAVY ACTIVITIES

Chief of Naval Operations, D/N, Washington 25, D. C.
ATTN: OP-36 — 86- 87
Chief of Naval Operations, D/N, Washington 25, D. C.
ATTN: OP-51 — 88
Chief of Naval Operations, D/N, Washington 25, D. C.
ATTN: OP-53 — 89
Chief of Naval Operations, D/N, Washington 25, D. C.
ATTN: OP-374 (CEG) — 90
Chief, Bureau of Medicine and Surgery, D/N, Washington 25, D. C. ATTN: Special Weapons Defense Division — 91- 92
Chief, Bureau of Ordnance, D/N, Washington 25, D. C. — 93
Chief, Bureau of Personnel, D/N, Washington 25, D. C.
ATTN: Pers 15 — 94
Chief, Bureau of Personnel, D/N, Washington 25, D. C.
ATTN: Pers C — 95
Chief, Bureau of Ships, D/N, Washington 25, D. C.
ATTN: Code 348 — 96

UNCLASSIFIED

UNCLASSIFIED

DISTRIBUTION (Continued)

	Copy No.
Chief, Bureau of Supplies and Accounts, D/N, Washington 25, D. C.	97
Chief, Bureau of Yards and Docks, D/N, Washington 25, D. C. ATTN: P-312	98
Chief, Bureau of Aeronautics, D/N, Washington 25, D. C.	99-100
Office of Naval Research, Code 219, Rm 1807, Bldg. T-3, Washington 25, D. C. ATTN: RD Control Officer	101
Commander-in-Chief, U. S. Atlantic Fleet, Fleet Post Office, New York, N. Y.	102-103
Commander-in-Chief, U. S. Pacific Fleet, Fleet Post Office, San Francisco, Calif.	104-105
Commander, Operation Development Force, U. S. Atlantic Fleet, U. S. Naval Base, Norfolk 11, Va. ATTN: Tactical Development Group	106
Commander, Operation Development Force, U. S. Atlantic Fleet, U. S. Naval Base, Norfolk 11, Va. ATTN: Air Department	107
Commandant, U. S. Marine Corps, Headquarters, USMC, Washington 25, D. C. ATTN: (A03H)	108-111
President, U. S. Naval War College, Newport, Rhode Island	112
Superintendent, U. S. Naval Postgraduate School, Monterey, Calif.	113
Commanding Officer, U. S. Naval Schools Command, Naval Station, Treasure Island, San Francisco, Calif.	114-115
Director, USMC Development Center, USMC Schools, Quantico, Va. ATTN: Marine Corps Tactics Board	116
Director, USMC Development Center, USMC Schools, Quantico, Va. ATTN: Marine Corps Equipment Board	117
Commanding Officer, Fleet Training Center, Naval Base, Norfolk 11, Va. ATTN: Special Weapons School	118-119
Commanding Officer, Fleet Training Center, (SPWP School), Naval Station, San Diego 36, Calif.	120-121
Commander, Air Force, U. S. Pacific Fleet, Naval Air Station, San Diego, Calif.	122
Commander, Training Command, U. S. Pacific Fleet, c/o Fleet Sonar School, San Diego 47, Calif.	123
Commanding Officer, Air Development Squadron 5, USN Air Station, Moffett Field, Calif.	124
Commanding Officer, Naval Damage Control Training Center, U. S. Naval Base, Philadelphia 12, Pa. ATTN: ABC Defense Course	125
Commanding Officer, Naval Unit, Chemical Corps School, Ft. McClellan, Ala.	126
Joint Landing Force Board, Marine Barracks, Camp Lejeune, N. C.	127

UNCLASSIFIED

[redacted]

DISTRIBUTION (Continued)

	Copy No.
Commander, U. S. Naval Ordnance Laboratory, Silver Spring 19, Md. ATTN: EE	128
Commander, U. S. Naval Ordnance Laboratory, Silver Spring 19, Md. ATTN: Alias	129
Commander, U. S. Naval Ordnance Laboratory, Silver Spring 19, Md. ATTN: Aliex	130
Commander, U. S. Naval Ordnance Test Station, Inyokern, China Lake, Calif.	131
Officer-in-Charge, U. S. Naval Civil Engineering Research and Evaluation Laboratory, Construction Battalion Center, Port Hueneme, Calif. ATTN: Code 753	132-133
Commanding Officer, USN Medical Research Institute, National Naval Medical Center, Bethesda 14, Md.	134
Director, U. S. Naval Research Laboratory, Washington 25, D. C.	135
Commanding Officer and Director, USN Electronics Laboratory, San Diego 52, Calif. ATTN: Code 210	136
Commanding Officer, USN Radiological Defense Laboratory, San Francisco, Calif. ATTN: Technical Information Division	137-138
Commanding Officer and Director, David W. Taylor Model Basin, Washington 7, D. C. ATTN: Library	139
Commander, Naval Air Development Center, Johnsville, Pa.	140
Commanding Officer, Office of Naval Research Branch Office, 1000 Geary St., San Francisco, Calif.	141-142

AIR FORCE ACTIVITIES

Special Asst. to Chief of Staff, Headquarters, USAF, Rm 5E1019, Pentagon, Washington 25, D. C.	143
Asst. for Atomic Energy, Headquarters, USAF, Washington 25, D. C. ATTN: DCS/O	144
Asst. for Development Planning, Headquarters, USAF, Washington 25, D. C.	145-146
Director of Operations, Headquarters, USAF, Washington 25, D. C.	147-148
Director of Plans, Headquarters, USAF, Washington 25, D. C. ATTN: War Plans Division	149
Directorate of Requirements, Headquarters, USAF, Washington 25, D. C. ATTN: AFDRQ-SA/M	150
Directorate of Research and Development, Armament Division, DCS/D, Headquarters, USAF, Washington 25, D. C.	151
Directorate of Intelligence, Headquarters, USAF, Washington 25, D. C.	152-153
The Surgeon General, Headquarters, USAF, Washington 25, D. C.	154-155

[redacted]

DISTRIBUTION (Continued)

	Copy No.
Commanding General, U. S. Air Forces Europe, APO 633, c/o PM, New York, N. Y.	156
Commanding General, Far East Air Forces, APO 925, c/o PM, San Francisco, Calif.	157
Commanding General, Alaskan Air Command, APO 942, c/o PM, Seattle, Wash. ATTN: AAOTN	158-159
Commanding General, Northeast Air Command, APO 862, c/o PM, New York, N. Y.	160
Commanding General, Strategic Air Command, Offutt AFB, Omaha, Neb. ATTN: Chief, Operations Analysis	161
Commanding General, Tactical Air Command, Langley AFB, Va. ATTN: Documents Security Branch	162-164
Commanding General, Air Defense Command, Ent AFB, Colo.	165-166
Commanding General, Air Material Command, Wright-Patterson AFB, Dayton, Ohio	167-169
Commanding General, Air Training Command, Scott AFB, Belleville, Ill.	170-171
Commanding General, Air Research and Development Command, PO Box 1395, Baltimore 3, Md. ATTN: RDDN	172-174
Commanding General, Air Proving Ground Command, Eglin AFB, Fla., ATTN: AG/THB	175
Commanding General, Air University, Maxwell AFB, Ala.	176-180
Commandant, Air Command and Staff School, Maxwell AFB, Ala.	181-182
Commandant, Air Force School of Aviation Medicine, Randolph AFB, Tex.	183-184
Commanding General, Wright Air Development Center, Wright-Patterson AFB, Dayton, Ohio. ATTN: WCOESP	185-190
Commanding General, Air Force Cambridge Research Center, 230 Albany St., Cambridge 39, Mass. ATTN: Atomic Warfare Directorate	191
Commanding General, Air Force Cambridge Research Center, 230 Albany St., Cambridge 39, Mass. ATTN: CRTSL-2	192
Commanding General, AF Special Weapons Center, Kirtland AFB, N. Mex. ATTN: Chief, Technical Library Branch	193-195
Commandant, USAF Institute of Technology, Wright-Patterson AFB, Dayton, Ohio. ATTN: Resident College	196
Commanding General, Lowry AFB, Denver, Colo. ATTN: Dept. of Armament Training	197-198
Commanding General, 1009th Special Weapons Squadron, 1712 G St., NW, Washington 25, D. C.	199-201
The RAND Corporation, 1500-4th St., Santa Monica, Calif. ATTN: Nuclear Energy Division	202-203

OTHER DEPT. OF DEFENSE ACTIVITIES

Executive Secretary, Joint Chiefs of Staff, Washington 25, D. C. ATTN: Joint Strategic Plans Committee	204

DISTRIBUTION (Continued)

	Copy No.
Director, Weapons Systems Evaluation Group, OSD, Rm 2E1006, Pentagon, Washington 25, D. C.	205
Asst. for Civil Defense, OSD, Washington 25, D. C.	206
Chairman, Armed Services Explosives Safety Board, D/D, Rm 2403, Barton Hall, Washington 25, D. C.	207
Chairman, Research and Development Board, D/D, Washington 25, D. C. ATTN: Technical Library	208
Executive Secretary, Committee on Atomic Energy, Research and Development Board, Rm 3E1075, Pentagon, Washington 25, D. C.	209-210
Executive Secretary, Military Liaison Committee, PO Box 1814, Washington 25, D. C.	211
Commandant, National War College, Washington 25, D. C. ATTN: Classified Records Section, Library	212
Commandant, Armed Forces Staff College, Norfolk 11, Va. ATTN: Secretary	213
Commanding General, Field Command, AFSWP, PO Box 5100, Albuquerque, N. Mex.	214-219
Chief, AFSWP, PO Box 2610, Washington 13, D. C.	220-228
University of California Radiation Laboratory, PO Box 808, Livermore, Calif. ATTN: Margaret Folden	229
Division of Military Application, U. S. Atomic Energy Commission, 1901 Constitution Ave., Washington 25, D. C.	230-232
Los Alamos Scientific Laboratory, Report Library, PO Box 1663, Los Alamos, N. Mex. ATTN: Helen Redman	233-235
Sandia Corporation, Classified Document Division, Sandia Base, Albuquerque, N. Mex. ATTN: Wynne K. Cox	236-255
Weapon Test Reports Group, TIS	256
Surplus in TISOR for AFSWP	257-305

AEC, Oak Ridge, Tenn., A-48279

END

FILMED

DATE:
5-96

DTIC